Electronic Supplementary Material (ESI) for New Journal of Chemistry.
This journal is © The Royal Society of Chemistry and the Centre National de la Recherche Scientifique 2016

Supporting Information

New Journal of Chemistry

Multipodal Arrangement of Push-Pull Chromophores: A Fundamental Parameter Affecting Their Electronic and Optical Properties

M. Klikar, I. V. Kityk, D. Kulwas, T. Mikysek, O. Pytela and F. Bureš

Table of contents

1. Synthesis and Characterization of Target Chromophores

Chromophore 1

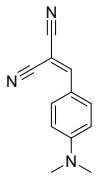

The title compound was synthesized via general method for Knoevenagel condensation (iii). Other preparation methods and spectral characterization is given in Ref.[1]. Chromophore **1** was synthesized from aldehyde **30** (170 mg; 1.141 mmol) and malondinitrile **25** (90 mg; 1.369 mmol) following the general method (iii). Yield: 150 mg (67 %); orange solid. R_f = 0.8 (SiO_2; CH_2Cl_2); mp 182 °C (lit.[1c] = 150 °C). Found: C, 72.98; H, 5.61; N, 21.20. $C_{12}H_{11}N_3$ requires C, 73.07; H, 5.62; N, 21.30 %. ^{1}H NMR ($CDCl_3$, 400 MHz; 25 °C): δ = 3.13 (s, 6H, NCH_3), 6.67 (d, J = 9.2 Hz, 2H, CHar), 7.43 (s, 1H, CH), 7.78 ppm (d, J = 9.2 Hz, 2H, CHar). ^{13}C NMR ($CDCl_3$, 100 MHz, 25 °C): δ = 40.3, 111.8, 115.1, 116.2, 119.5, 134.0, 154.5, 158.2 ppm. HR-MALDI-MS (DHB): calcd for $C_{12}H_{11}N_3$ (M^+) 197.09475 found 197.09481.

Chromophore 2

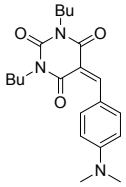

The title compound was synthesized via general method for Knoevenagel condensation (iii). Spectral characterization is given in Ref.[2]. Chromophore **2** was synthesized from aldehyde **30** (149 mg; 1.0 mmol) and *N,N´*-dibutylbarbituric acid **26** (288 mg; 1.2 mmol) following the general method (iii). Yield: 300 mg (81 %); orange-red solid. R_f = 0.7 (SiO_2; CH_2Cl_2); mp 163 °C (lit.[2] = 156-161 °C). Found: C, 67.85; H, 8.00; N, 11.09. $C_{21}H_{29}N_3O_3$ requires C, 67.90; H, 7.87; N, 11.31 %. ^{1}H NMR ($CDCl_3$, 400 MHz; 25 °C): δ = 0.92-0.96 (m, 6H, CH_3), 1.34-1.40 (m, 4H, CH_2), 1.60-1.64 (m, 4H, CH_2), 3.13 (s, 6H, NCH_3), 3.94-3.98 (m, 4H, CH_2), 6.69 (d, J = 9.2 Hz, 2H, CHar), 8.37 (d, J = 9.2 Hz, 2H, CHar), 8.42 ppm (s, 1H, CH). ^{13}C NMR ($CDCl_3$, 100 MHz, 25 °C): δ = 14.01, 14.04, 20.41, 20.47, 30.43, 30.46, 40.3, 41.7, 42.3, 110.3, 111.2, 121.3, 139.6, 151.5, 154.5, 158.9, 161.6, 164.0 ppm. HR-MALDI-MS (DHB): calcd for $C_{21}H_{30}N_3O_3$ $(M+H)^+$ 372.22817 found 372.22775.

Chromophore 3

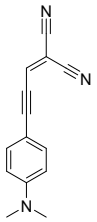

The title compound was synthesized via general method for Knoevenagel condensation (iii). Spectral characterization is given in Ref.[3]. Chromophore **3** was synthesized from aldehyde **49** (65 mg; 0.376 mmol) and malondinitrile **25** (30 mg; 0.451 mmol) following the general method (iii). Yield: 62 mg (75 %); violet solid. R_f = 0.8 (SiO_2; CH_2Cl_2); mp 131 °C (lit.[3] = 130-131 °C). Found: C, 75.97; H, 4.95; N, 18.84. $C_{14}H_{11}N_3$ requires C, 76.00; H, 5.01; N, 18.99 %. ^{1}H NMR ($CDCl_3$, 400 MHz; 25 °C): δ = 3.07 (s, 6H, NCH_3), 6.63 (d, J = 9.2 Hz, 2H, CHar), 7.08 (s, 1H, CH), 7.46 ppm (d, J = 9.2 Hz, 2H, CHar). ^{13}C NMR ($CDCl_3$, 100 MHz, 25 °C): δ = 40.2, 88.3, 88.5, 105.9, 111.9, 112.6, 113.8, 135.8, 141.3, 152.8 ppm. HR-MALDI-MS (DHB): calcd for $C_{14}H_{11}N_3$ (M^+) 221.09475 found 221.09480.

Chromophore 4

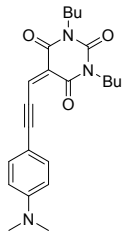

The title compound was synthesized via general method for Knoevenagel condensation (iii). Spectral characterization is given in Ref.[2]. Chromophore **4** was synthesized from aldehyde **49** (173 mg; 1.0 mmol) and *N,N´*-dibutylbarbituric acid **26** (288 mg; 1.2 mmol) following the general method (iii). Yield: 304 mg (77 %); violet solid. R_f = 0.7 (SiO_2; CH_2Cl_2); mp 143 °C (lit.[2] = 144-148 °C). Found: C, 70.00; H, 7.52; N, 10.51. $C_{23}H_{29}N_3O_3$ requires C, 69.85; H, 7.39; N, 10.62 %. ^{1}H NMR ($CDCl_3$, 400 MHz; 25 °C): δ = 0.92-0.97 (m, 6H, CH_3), 1.33-1.41 (m, 4H, CH_2), 1.58-1.65 (m, 4H, CH_2), 3.07 (s, 6H, NCH_3), 3.91-3.95 (m, 4H, CH_2), 6.65 (d, J = 8.8 Hz, 2H, CHar), 7.58 (d, J = 8.8 Hz, 2H, CHar), 7.81 ppm (s, 1H, CH). ^{13}C NMR ($CDCl_3$, 100 MHz, 25 °C): δ = 13.96, 13.98, 20.36, 20.41, 30.3, 40.2, 41.6, 42.1, 94.0, 108.0, 111.8, 121.6, 125.6, 136.3, 137.4, 151.2, 152.5, 159.9, 161.9 ppm. HR-MALDI-MS (DHB): calcd for $C_{23}H_{30}N_3O_3$ $(M+H)^+$ 396.22817 found 396.22717.

Chromophore 9

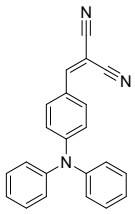

The title compound was synthesized via general method for Knoevenagel condensation (iii). Other preparation methods and spectral characterization is given in Ref.[4]. Chromophore **9** was synthesized from aldehyde **32** (273 mg; 1.0 mmol) and malondinitrile **25** (79 mg; 1.2 mmol) following the general method (iii). Yield: 285 mg (89 %); orange solid. R_f = 0.8 (SiO_2; CH_2Cl_2); mp 139 °C (lit.[4c] = 196-197 °C). Found: C, 82.16; H, 4.72; N, 13.07. $C_{22}H_{15}N_3$ requires C, 82.22; H, 4.70; N, 13.08 %. ^{1}H NMR ($CDCl_3$, 400 MHz; 25 °C): δ = 6.94 (d, J = 8.8 Hz, 2H, CHar), 7.18-7.25 (m, 6H, CHar), 7.36-7.40 (m, 4H, CHar), 7.51 (s, 1H, CH), 7.73 ppm (d, J = 9.2 Hz, 2H, CHar). ^{13}C NMR ($CDCl_3$, 100 MHz, 25 °C): δ = 114.3, 115.4, 118.7, 123.0, 126.3, 126.9, 130.2, 133.2, 145.4, 153.7, 158.1 ppm. HR-MALDI-MS (DHB): calcd for $C_{22}H_{15}N_3$ (M^+) 321.12605 found 321.12579.

Chromophore 17

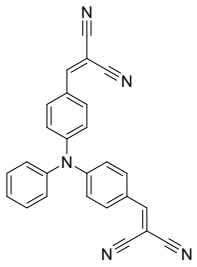

The title compound was synthesized via general method for Knoevenagel condensation (iii). Other preparation methods and spectral characterization is given in Ref.[4b,5]. Chromophore **17** was synthesized from aldehyde **34** (301 mg; 1.0 mmol) and malondinitrile **25** (158 mg; 2.4 mmol) following the general method (iii). Yield: 310 mg (78 %); terracotta solid. R_f = 0.55 (SiO_2; CH_2Cl_2); mp 226 °C (lit.[5] = 228-232 °C). Found: C, 78.54; H, 3.83; N, 17.59. $C_{26}H_{15}N_5$ requires C, 78.57; H, 3.80; N, 17.62 %. ^{1}H NMR ($CDCl_3$, 400 MHz; 25 °C): δ = 7.17 (d, J = 8.8 Hz, 6H, CHar), 7.31-7.36 (m, 1H, CHar), 7.41-7.46 (m, 2H, CHar), 7.62 (s, 2H, CH), 7.83 ppm (d, J = 8.8 Hz, 4H, CHar). ^{13}C NMR ($CDCl_3$, 100 MHz, 25 °C): δ = 113.5, 114.5, 123.0, 126.1, 127.6, 127.7, 130.8, 132.9, 144.5, 151.5, 158.0 ppm. HR-MALDI-MS (DHB): calcd for $C_{26}H_{15}N_5$ (M^+) 397.13220 found 397.13244.

Chromophore 21

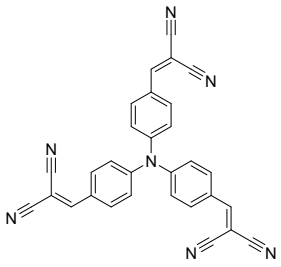

The title compound was synthesized via general method for Knoevenagel condensation (iii). Other preparation methods and spectral characterization is given in Ref.[4b,5,6]. Chromophore **21** was synthesized from aldehyde **35** (200 mg; 0.608 mmol) and malondinitrile **25** (145 mg; 2.189 mmol) following the general method (iii). Column chromatography was 3 times repeated (CH_2Cl_2/acetone 45:5). Yield: 120 mg (42 %); orange solid. R_f = 0.4 (SiO_2; CH_2Cl_2); mp 218 °C (lit.[5] = 192-193 °C). Found: C, 76.31; H, 3.26; N, 20.61. $C_{30}H_{15}N_7$ requires C, 76.10; H, 3.19; N, 20.71 %. ^{1}H NMR ($CDCl_3$, 400 MHz; 25 °C): δ = 7.24 (d, J = 8.4 Hz, 6H, CHar), 7.69 (s, 3H, CH), 7.91 ppm (d, J = 8.8 Hz, 6H, CHar). ^{13}C NMR ($CDCl_3$, 100 MHz, 25 °C): δ = 113.0, 114.0, 125.1, 127.9, 133.0, 150.3, 157.7 ppm. HR-MALDI-MS (DHB): calcd for $C_{30}H_{15}N_7$ (M^+) 473.13835 found 473.13855.

Chromophore 23

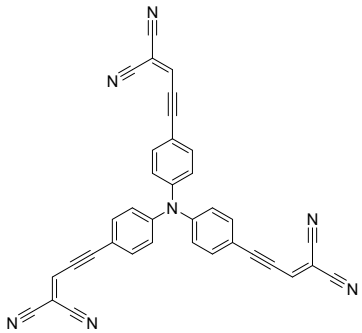

The title compound was synthesized via general method for Knoevenagel condensation (iii). Spectral characterization is given in Ref.[6b]. Chromophore **23** was synthesized from aldehyde **54** (100 mg; 0.249 mmol) and malondinitrile **25** (59 mg; 0.897 mmol) following the general method (iii). Yield: 95 mg (70 %); red-violet solid. R_f = 0.7 (SiO_2; CH_2Cl_2). Found: C, 78.42; H, 2.78.; N, 17.85. $C_{35}H_{15}N_7$ requires C, 79.26; H, 2.77; N, 17.97 %. ^{1}H NMR ($CDCl_3$, 400 MHz; 25 °C): δ = 7.12-7.16 (m, 9H, CHar+CH), 7.55 ppm (d, J = 8.8 Hz, 6H, CHar). ^{13}C NMR ($CDCl_3$, 100 MHz, 25 °C): δ = 86.5, 93.4, 111.7, 112.7, 115.1, 115.9, 124.7, 135.2, 141.0, 148.8 ppm. HR-MALDI-MS (DHB): calcd for $C_{36}H_{15}N_7$ (M^+) 545.13835 found 545.13860.

2. Synthesis and Characterization of Intermediates

2.1. Iodination of starting compounds

Iodo derivatives 28-29

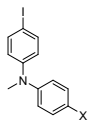
28, X = H
29, X = I

A mixture of compounds **28-29** was synthesized via modified literature procedure.[7] Namely, $AgNO_3$ (927 mg, 5.46 mmol) was dissolved in glycerine (20 mL) using ultrasound bath. This solution was diluted by EtOH (200 mL, 96 %) whereupon **27** (1.0 g, 5.46 mmol) and I_2 (1.39 g, 5.46 mmol) were added and the reaction mixture was stirred at 25 °C for 1 hour. The reaction mixture was filtered through a Celite plug and the filtrate was concentrated *in vacuo*. The resulting solution in glycerine was dissolved in CH_2Cl_2 (200 mL) and extracted by aqueous solution of Na_2SO_3 (2 × 50 mL) and H_2O (2 × 50 mL). The organic layer was dried (Na_2SO_4), filtered, and the solvent was removed *in vacuo*. A mixture of **28** (44 %) and **29** (32 %) was obtained as viscous oil with the overall yield of 1.49 g. These yields were roughly estimated from the peak areas of the corresponding GC spectrum. This mixture was used in the next reaction steps without further purification. EI/MS (70 eV): *m/z* 309 (M^+, 100 %), 181 (16), 167 (31), 91 (9), 77 (11) for **28** and *m/z* 435 (M^+, 100 %), 207 (62), 180 (33), 166 (32), 76 (19) for **29**.

4-Iodo-*N*,*N*-dimethylaniline 37

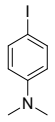

The title compound was synthesized via modified literature procedure.[8] Into a mixture of *N*,*N*-dimethylaniline **36** (12.12 g, 0.1 mol) and $NaHCO_3$ (12.60 g, 0.15 mol) in water (100 mL) I_2 (22.9 g, 0.09 mol) was gradually added with vigorous stirring. The reaction mixture was kept at 25 °C for 3 hours, diluted with CH_2Cl_2 (250 mL), intensively blue organic layer was separated, and washed with Na_2SO_3 (100 mL). The organic layer was dried (Na_2SO_4) and the solvent was evaporated *in vacuo*. The crude blue product was crystalized three times from EtOH/H_2O and washed by cold EtOH. Yield: 14.1 g (57 %); off-white solid. EI/MS (70 eV): *m/z* 247 (M^+, 100 %), 119 (15), 105 (10), 77 (12).

Iodo derivatives 40-41

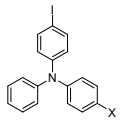
40, X = H
41, X = I

The mixture of compounds **40-41** was synthesized following the same procedure as for **28**-**29** starting from **39** (736 mg, 3.0 mmol). A mixture of **40** (50 %) and **41** (25 %) was obtained as pale yellow viscous oil with the overall yield of 820 mg. These yields were roughly estimated from the peak areas of the corresponding GC spectrum. This mixture was used in the next reaction steps without further purification. EI/MS (70 eV): *m/z* 371 (M^+, 100 %), 243 (36), 167 (32), 139 (14), 122 (14), 77 (21) for **40** and *m/z* 497 (M^+, 100 %), 370 (11), 242 (62), 166 (25), 139 (26), 76 (27) for **41**.

Iodo derivatives 42

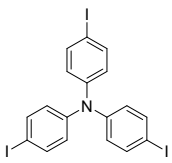

The title compound **42** was synthesized following the same procedure as for **28**-**29** starting from **39** (736 mg, 3.0 mmol) and I_2 (2.3 g, 9 mmol). Yield: 1.64 g pale yellow, amorphous solid. ^{1}H NMR ($CDCl_3$, 400 MHz; 25 °C): δ = 6.80 (d, *J* = 8.8 Hz, 6H, CHar), 7.52 ppm (d, *J* = 8.8 Hz, 6H, CHar). ^{13}C NMR ($CDCl_3$, 100 MHz, 25 °C): δ = 86.8, 126.3, 138.7, 146.8 ppm.

2.2. Formylations

Aldehyde 31

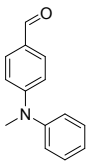

The title compound **31** was synthesized via literature procedure.[9a] *n*Buli (4.71 mL, 7.54 mmol) was added slowly to a solution of iodinated mixture of **28-29** (1.49 g, ca. 1:1 mixture) in dry THF (20 mL) at -78 °C under argon and the reaction mixture was stirred for 1.5 h. Dry DMF (0.58 mL, 7.54 mmol) was added, the reaction was allowed to reach 25 °C, and was stirred additional 1 h. The reaction mixture was poured into a stirred mixture of K_2HPO_4 (50 mL, sat. aq.) and 50 mL Et_2O, the organic phase was separated, and the water layer was extracted with ether (50 mL). The combined organic extracts were dried (Na_2SO_4), the solvents were evaporated *in vacuo*, and the residue was purifying by

column chromatography (SiO_2; CH_2Cl_2) to afford desired aldehyde **31**. Aldehyde **33** was discarded as a side product (commercially available). Yield: 410 mg (80 %, based on the amount of **28** in the starting mixture **28**-**29**); yellow, amorphous solid. R_f = 0.5 (SiO_2; CH_2Cl_2). EI/MS (70 eV): *m/z* 211 (M^+, 100 %), 180 (9), 167 (35), 139 (14), 77 (24), 51 (11). ^{1}H NMR ($CDCl_3$, 400 MHz; 25 °C): δ = 3.36 (s, 3H, NCH_3), 6.76 (d, *J* = 8.8 Hz, 2H, CHar), 7.20-7.27 (m, 3H, CHar), 7.39-7.43 (m, 2H, CHar), 7.67 (d, *J* = 8.8 Hz, 2H, CHar), 9.74 ppm (s, 1H, CHO). ^{13}C NMR ($CDCl_3$, 100 MHz, 25 °C): δ = 40.4, 113.5, 126.3, 126.6, 126.7, 130.1, 131.7, 146.9, 153.8, 190.4 ppm. The measured analytical data were in accordance with those published in literature.[9b]

2.3. Sonogashira Cross-Coupling Reactions

Alcohol 43

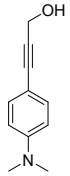

Iodo derivative **37** (370 mg, 1.5 mmol) and propargyl alcohol **38** (101 mg, 1.8 mmol) were cross-coupled following the general method (i). Yield: 176 mg (67 %); brown oil. R_f = 0.8 (SiO_2; CH_2Cl_2/EtOAc 3:1). EI/MS (70 eV): *m/z* 175 (M^+, 100 %), 158 (45), 148 (28), 144 (42), 120 (16). ^{1}H NMR ($CDCl_3$, 400 MHz; 25 °C): δ = 1.65 (t, *J* = 5.6 Hz, 1H, OH), 2.96 (s, 6H, NCH_3), 4.48 (d, *J* = 5.6 Hz, 2H, CH_2), 6.61 (d, *J* = 8.8 Hz, 2H, CHar), 7.31 ppm (d, *J* = 8.8 Hz, 2H, CHar). ^{13}C NMR ($CDCl_3$, 100 MHz, 25 °C): δ = 40.4, 52.1, 85.2, 87.0, 109.4, 111.9, 133.0, 150.4 ppm. The measured analytical data were in accordance with those published in literature.[2]

Alcohols 44 and 46

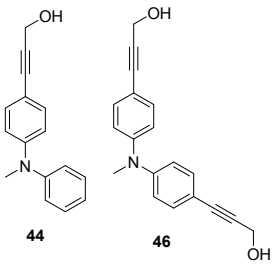

44 **46**

Mixture of **28**-**29** (1.49 g, ca. 1:1) and propargyl alcohol **38** (420 mg, 7.5 mmol) were cross-coupled following the general method (i). Both alcohols were separated by column chromatography (SiO_2; CH_2Cl_2/EtOAc 3:1). Yield of **44**: 422 mg (74 % relative to 1:1 starting mixture); brown solid. R_f = 0.8 (SiO_2; CH_2Cl_2/EtOAc 3:1). ^{1}H NMR ($CDCl_3$, 400 MHz; 25 °C): δ = 1.65 (t, *J* = 6.0 Hz, 1H, OH), 3.29 (s, 3H, NCH_3), 4.45 (d, *J* = 6.0 Hz, 2H, CH_2), 6.77 (d, *J* = 8.8 Hz, 2H, CHar), 7.06-7.12 (m, 2H, CHar), 7.23-7.33 ppm (m, 5H, CHar). Yield of **46**: 345 mg (68 % relative to 1:1 starting mixture); brownish solid. R_f = 0.6 (SiO_2; CH_2Cl_2/EtOAc 3:1). ^{1}H NMR ($CDCl_3$, 400 MHz; 25 °C): δ = 1.66 (t, *J* = 6.0 Hz, 2H, OH), 3.31 (s, 3H, NCH_3), 4.48 (d, *J* = 6.0 Hz, 4H, CH_2), 6.95 (dd, J_1 = 6.8 Hz, J_2 = 2Hz, 4H, CHar), 7.32 ppm (dd, ^1J = 6.8 Hz, ^2J = 2Hz, 4H, CHar). ^{13}C NMR ($CDCl_3$, 100 MHz, 25 °C): δ = 40.2, 52.0, 86.0, 86.5, 115.4, 120.3, 133.1, 148.5 ppm.

Alcohols 45 and 47

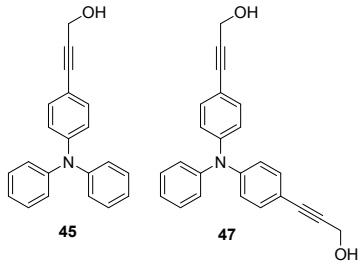

45 **47**

Mixture of **40**-**41** (800 mg, ca. 3:2 mixture) and propargyl alcohol **38** (180 mg, 3.23 mmol) were cross-coupled following the general method (i). Both alcohols were separated by column chromatography. Yield of **45**: 340 mg (88 % relative to 3:2 starting mixture); brown viscous oil. R_f = 0.9 (SiO_2; CH_2Cl_2/EtOAc 3:1). ^{1}H NMR ($CDCl_3$, 400 MHz; 25 °C): δ = 1.74 (t, *J* = 5.6 Hz, 1H, OH), 4.48 (d, *J* = 5.6 Hz, 2H, CH_2), 6.94-6.97 (m, 2H, CHar), 7.03-7.10 (m, 6H, CHar), 7.24-7.28 ppm (m, 6H, CHar). ^{13}C NMR ($CDCl_3$, 100 MHz, 25 °C): δ = 52.0, 86.1, 86.5, 115.5, 122.3, 123.8, 125.2, 129.9, 132.9, 147.4, 148.4 ppm. The measured NMR spectra were in accordance with those published in literature.[10] Yield of **47**: 160 mg (70 % relative to 3:2 starting mixture); brown viscous oil. R_f = 0.55 (SiO_2; CH_2Cl_2/EtOAc 3:1). ^{1}H NMR ($CDCl_3$, 400 MHz; 25 °C): δ = 1.74 (s, 2H, OH), 4.48 (s, 4H, CH_2), 6.97 (d, *J* = 8.4 Hz, 4H, CHar), 7.07-7.09 (m, 3H, CHar), 7.25-7.30 ppm (m, 6H, CHar). ^{13}C NMR ($CDCl_3$, 100 MHz, 25 °C): δ = 51.9, 85.9, 86.9, 116.5, 123.4, 124.5, 125.8, 129.8, 133.0, 146.8, 147.6 ppm.

Alcohol 48

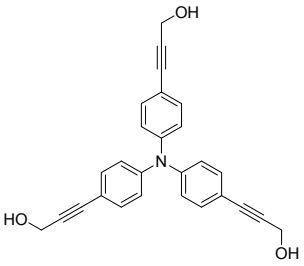

Iodo derivative **42** (935 mg, 1.5 mmol) and propargyl alcohol **38** (356 mg, 5.4 mmol) were cross-coupled following the general method (i). Yield: 510 mg (83 %); brownish solid. R_f = 0.5 (SiO_2; CH_2Cl_2/EtOAc 1:1). ^{1}H NMR ($CDCl_3$, 400 MHz; 25 °C): δ = 2.68 (s, 3H, OH), 4.48 (s, 6H, CH_2), 6.98 (d, J = 8.8 Hz, 6H, CHar), 7.31 ppm (d, J = 8.8 Hz, 6H, CHar). ^{13}C NMR ($CDCl_3$, 100 MHz, 25 °C): δ = 51.9, 85.7, 87.2, 117.4, 124.1, 133.1, 147.0 ppm. The measured NMR spectra were in accordance with those published in literature.[6b]

2.4. Dess-Martin Oxidations

Aldehyde 49

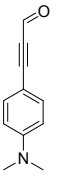

Alcohol **43** (50 mg, 0.29 mmol) was treated with Dess-Martin periodinane (121 mg, 0.29 mmol) following general method (ii). Yield: 38 mg (76 %); yellow-orange solid. R_f = 0.8 (SiO_2; CH_2Cl_2). ^{1}H NMR ($CDCl_3$, 400 MHz, 25 °C): δ = 3.03 (s, 6H, NCH_3), 6.63 (d, 2H, J = 8,8 Hz, CH ar.), 7.47 (d, 2H, J = 8,8 Hz, CH ar.), 9.35 (s, 1H,CH=O). ^{13}C NMR ($CDCl_3$, 100 MHz, 25 °C): δ = 40.19, 90.34, 100.35, 104.96, 111.74, 135.66, 152.26, 176.72. The measured analytical data were in accordance with those published in literature.[11]

Aldehyde 50

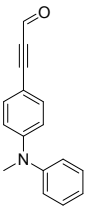

Alcohol **44** (200 mg, 0.84 mmol) was tretaed with Dess-Martin periodinane (356 mg, 0.84 mmol) following general method (ii). Yield: 160 mg (81 %); yellow viscous oil. R_f = 0.8 (SiO_2; CH_2Cl_2). ^{1}H NMR ($CDCl_3$, 400 MHz; 25 °C): δ = 3.35 (s, 3H, NCH_3), 6.72 (d, J = 8.8 Hz, 2H, CHar), 7.19-7.23 (m, 3H, CHar), 7.39-7.44 (m, 4H, CHar), 9.36 ppm (s, 1H, CHO).

Aldehyde 51

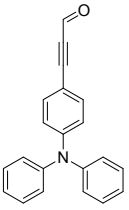

Alcohol **45** (290 mg, 0.97 mmol) was treated with Dess-Martin periodinane (411 mg, 0.97 mmol) following general method (ii). Yield: 170 mg (59 %); yellow-brown viscous oil. R_f = 0.8 (SiO_2; CH_2Cl_2). ^{1}H NMR ($CDCl_3$, 400 MHz; 25 °C): δ = 6.94 (dd, J_1 = 7.2 Hz, J_2 = 2 Hz, 2H, CHar), 7.12-7.15 (m, 6H, CHar), 7.29-7.33 (m, 4H, CHar), 7.41 (dd, J_1 = 7.2 Hz, J_2 = 2 Hz, 2H, CHar), 9.37 ppm (s, 1H, CHO). ^{13}C NMR ($CDCl_3$, 100 MHz, 25 °C): 89.6, 97.9, 110.4, 120.3, 125.0, 126.2, 129.9, 135.1, 146.4, 151.0, 176.9 ppm. The measured NMR spectra were in accordance with those published in literature.[10]

Aldehyde 52

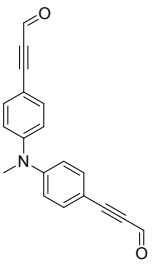

Alcohol **46** (160 mg, 0.55 mmol) was treated with Dess-Martin periodinane (467 mg, 1.1 mmol) following general method (ii). Yield: 130 mg (82 %); yellow solid. R_f = 0.7 (SiO_2; CH_2Cl_2). ^{1}H NMR ($CDCl_3$, 400 MHz; 25 °C): δ = 3.41 (s, 3H, NCH_3), 7.06 (dd, J_1 = 8.8 Hz, J_2 = 2 Hz, 4H, CHar), 7.53 (dd, J_1 = 8.8 Hz, J_2 = 2 Hz, 4H, CHar), 9.39 ppm (s, 2H, CHO). ^{13}C NMR ($CDCl_3$, 100 MHz, 25 °C): 40.2, 89.5, 96.6, 112.3, 120.6, 135.3, 150.1, 176.9 ppm.

Aldehyde 53

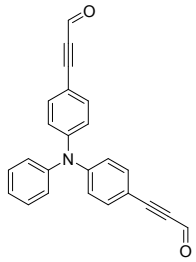

Alcohol **47** (140 mg, 0.4 mmol) was treated with Dess-Martin periodinane (336 mg, 0.8 mmol) following general method (ii). Yield: 101 mg (72 %); yellow viscous oil. R_f = 0.7 (SiO_2; CH_2Cl_2). ^{1}H NMR ($CDCl_3$, 400 MHz; 25 °C): δ = 7.06 (d, J = 8.8 Hz, 4H, CHar), 7.13 (d, J = 7.6 Hz, 2H, CHar), 7.20-7.24 (m, 1H, CHar), 7.34-7.38 (m, 2H, CHar), 7.48 (d, J = 8.8 Hz, 4H, CHar), 9.39 ppm (s, 2H, CHO). ^{13}C NMR ($CDCl_3$, 100 MHz, 25 °C): 89.4, 96.2, 113.2, 123.1, 126.2, 126.9, 130.3, 135.1, 145.6, 149.5, 176.8 ppm.

Aldehyde 54

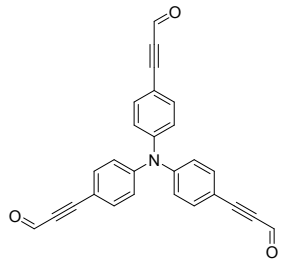

Alcohol **4** (250 mg, 0.61 mmol) was treated with Dess-Martin periodinane (781 mg, 1.84 mmol) following general method (ii). Yield: 205 mg (83 %); yellow solid. R_f = 0.6 (SiO_2; CH_2Cl_2). ^{1}H NMR ($CDCl_3$, 400 MHz; 25 °C): δ = 7.10 (d, J = 8.4 Hz, 6H, CHar), 7.52 (d, J = 8.4 Hz, 6H, CHar), 9.37 ppm (s, 3H, CHO). ^{13}C NMR ($CDCl_3$, 100 MHz, 25 °C): 89.3, 95.2, 114.9, 124.5, 135.2, 148.5, 176.7 ppm. The NMR spectra were in accordance with those published in literature.[6b]

3. Electrochemistry

Electrochemical measurements of chromophores **1-24** were carried out in *N*,*N*-dimethylformamide containing 0.1 M Bu_4NPF_6 in a three electrode cell by cyclic voltammetry (CV), rotating disk voltammetry (RDV) and polarography. The working electrode was platinum disk (2 mm in diameter) for CV and RDV experiments. Saturated calomel electrode (SCE) separated by a bridge filled with supporting electrolyte and Pt wire were used as reference and auxiliary electrodes. Voltammetric measurements were performed using a potentiostat PGSTAT 128N (AUTOLAB, Metrohm Autolab B.V., Utrecht, The Netherlands) operated via NOVA 1.10 software.

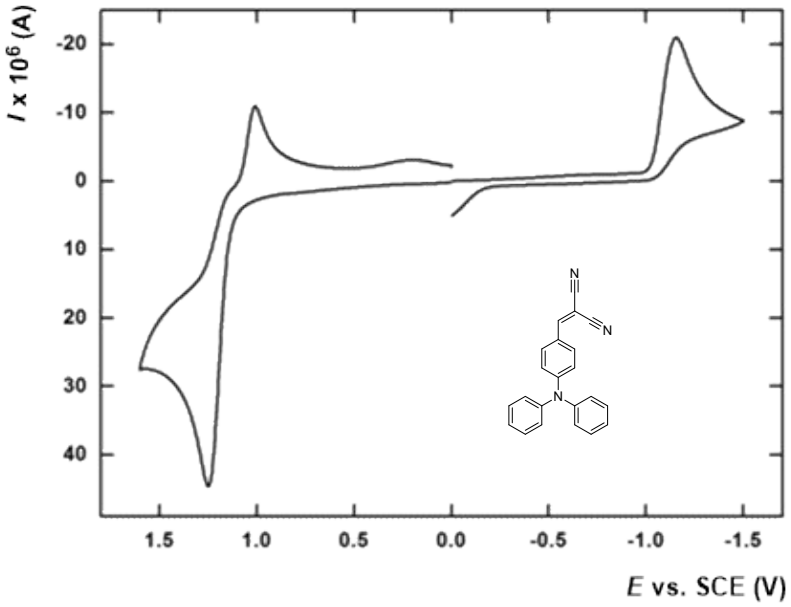

Figure S1. Representative CV curve of the oxidation and reduction of chromophore **9** at Pt electrode in DMF containing 0.1 M Bu_4NPF_6, scan rate 100 $mV.s^{-1}$.

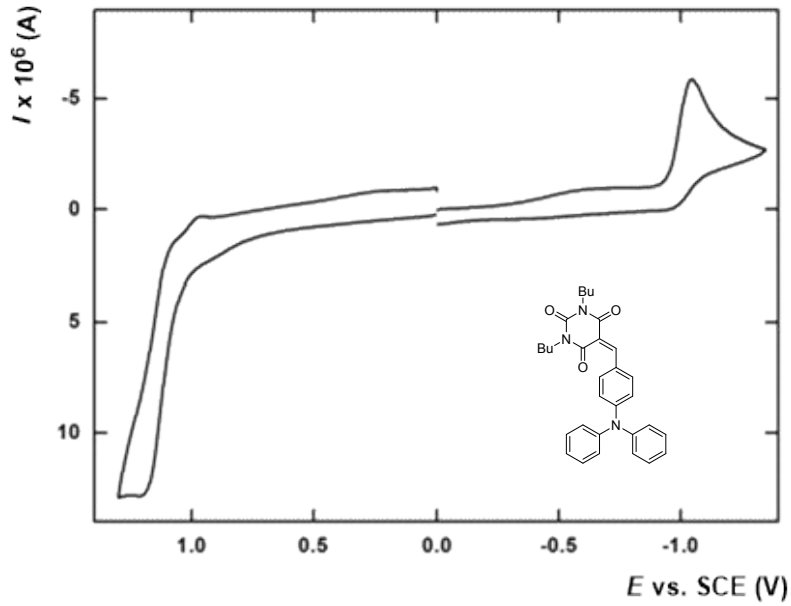

Figure S2. Representative CV curve of the oxidation and reduction of chromophore **10** at Pt electrode in DMF containing 0.1 M Bu_4NPF_6, scan rate 100 $mV.s^{-1}$.

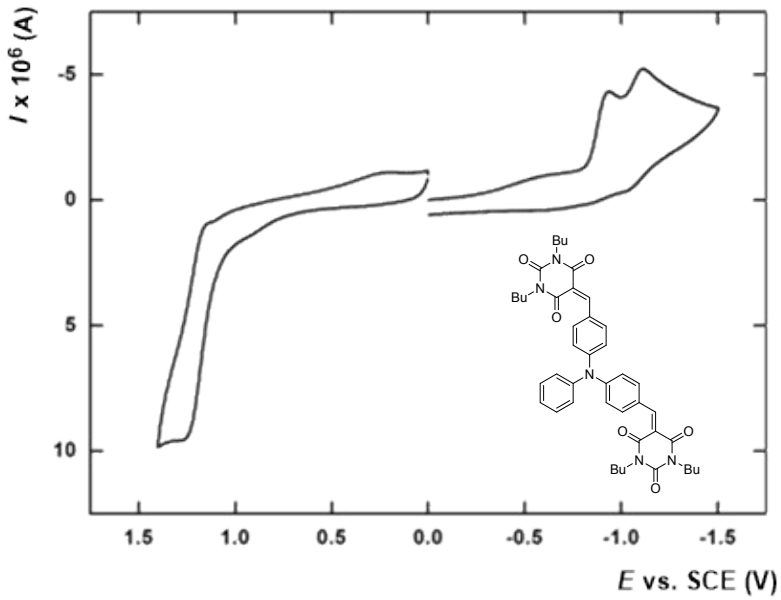

Figure S3. Representative CV curve of the oxidation and reduction of chromophore **18** at Pt electrode in DMF containing 0.1 M Bu_4NPF_6, scan rate 100 $mV.s^{-1}$.

4. Optical properties

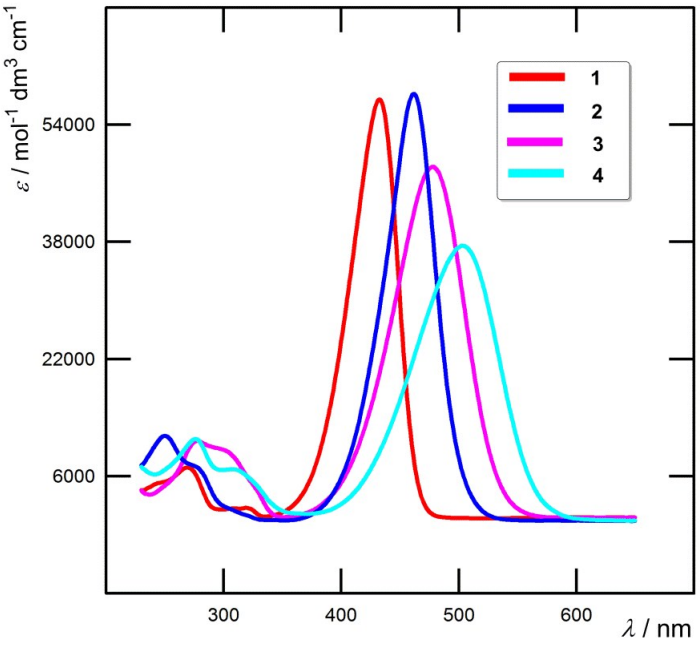

Figure S4. UV-Vis absorption spectra of linear chromophores **1-4** (Me_2N donor) measured in CH_2Cl_2 ($2 \cdot 10^{-5}$ M).

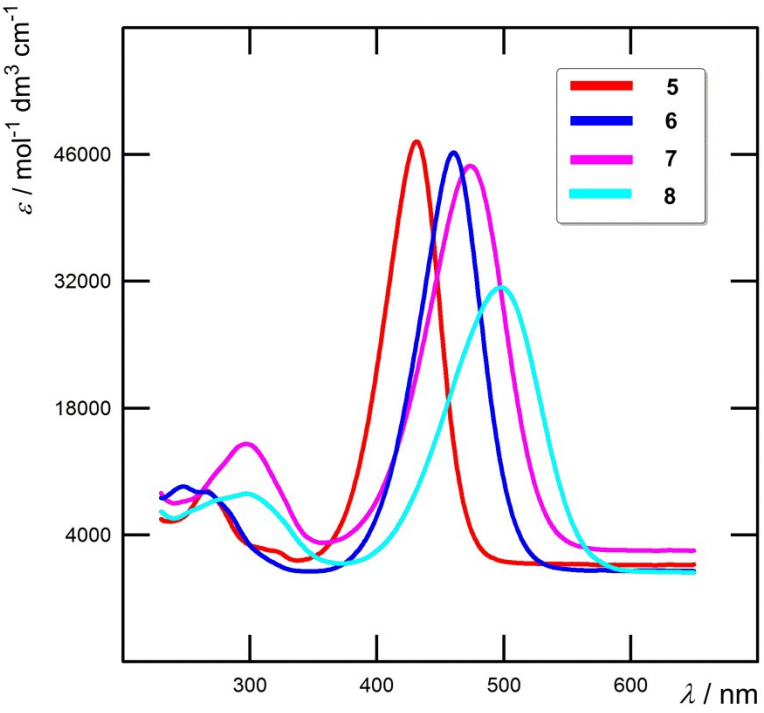

Figure S5. UV-Vis absorption spectra of linear chromophores **5-8** (MePhN donor) measured in CH_2Cl_2 ($2 \cdot 10^{-5}$ M).

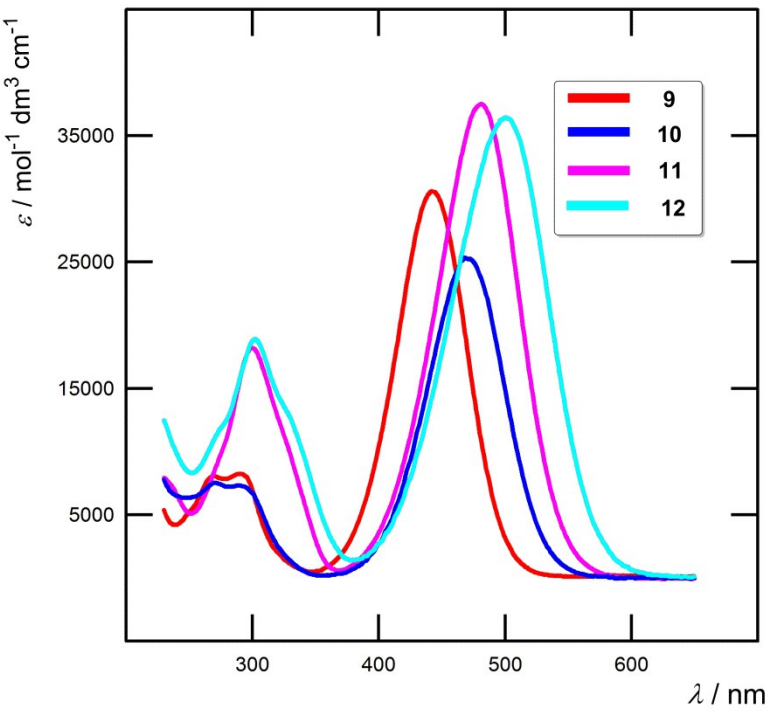

Figure S6. UV-Vis absorption spectra of linear chromophores **9-12** (Ph_2N donor) measured in CH_2Cl_2 ($2 \cdot 10^{-5}$ M).

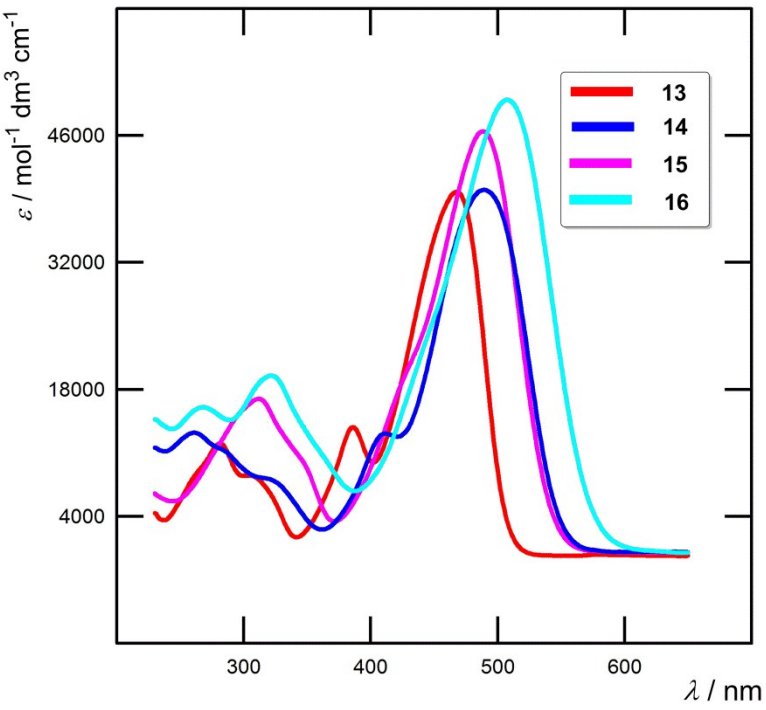

Figure S7. UV-Vis absorption spectra of quadrupolar chromophores **13-16** (MeN donor) measured in CH_2Cl_2 ($2 \cdot 10^{-5}$ M).

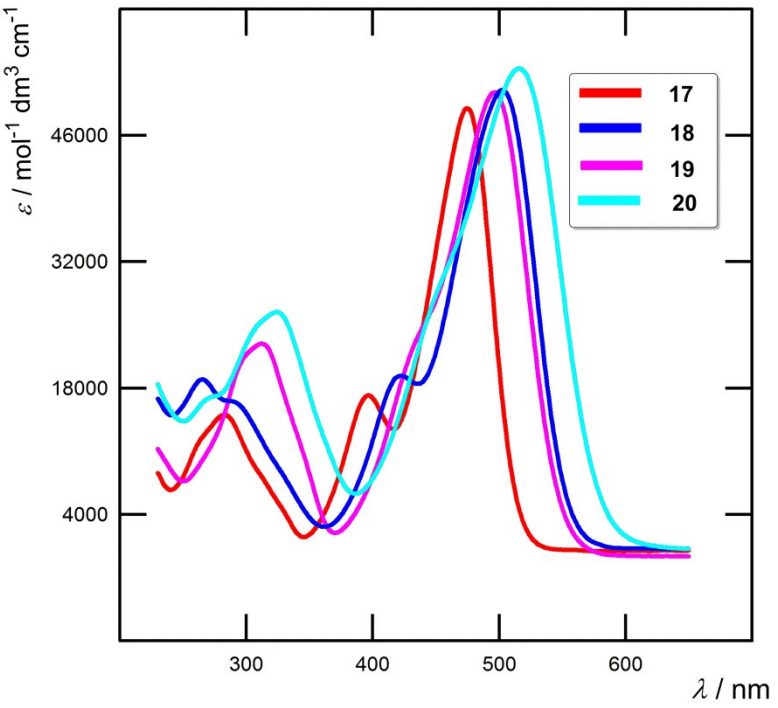

Figure S8. UV-Vis absorption spectra of quadrupolar chromophores **17-20** (PhN donor) measured in CH_2Cl_2 ($2 \cdot 10^{-5}$ M).

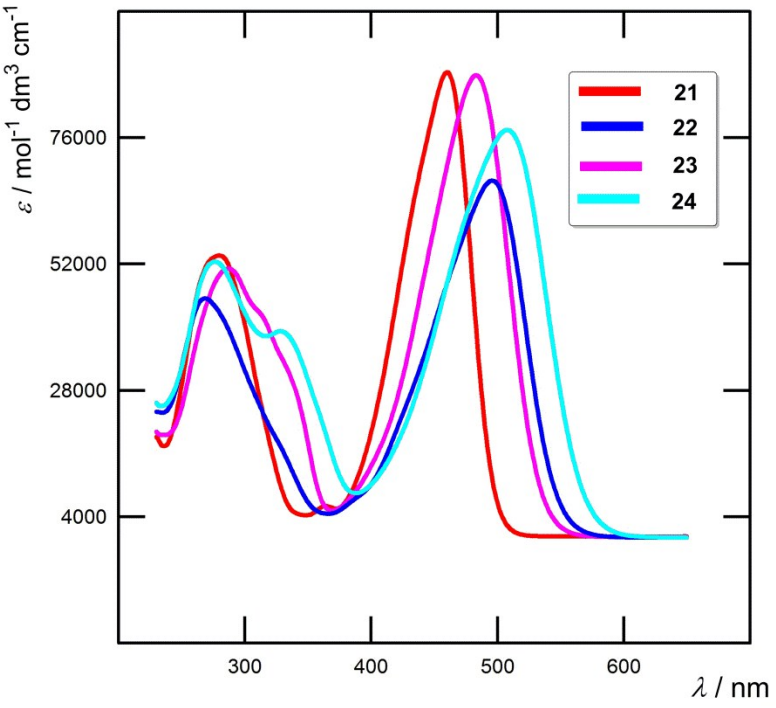

Figure S9. UV-Vis absorption spectra of tripodal chromophores **21-24** measured in CH_2Cl_2 ($2 \cdot 10^{-5}$ M).

Table 1. Solvatochromic data of chromophores **12**, **20**, and **24**.

	Toluene		THF		CH_2Cl_2		DMSO		Acetonitrile		MeOH	
Comp.	$\lambda_{max}{}^{A}$ (nm)	$\varepsilon_{max}{}^{A}$ ($M^{-1}\cdot cm^{-1}$)	$\lambda_{max}{}^{A}$ (nm)	$\varepsilon_{max}{}^{A}$ ($M^{-1}\cdot cm^{-1}$)	$\lambda_{max}{}^{A}$ (nm)	$\varepsilon_{max}{}^{A}$ ($M^{-1}\cdot cm^{-1}$)	$\lambda_{max}{}^{A}$ (nm)	$\varepsilon_{max}{}^{A}$ ($M^{-1}\cdot cm^{-1}$)	$\lambda_{max}{}^{A}$ (nm)	$\varepsilon_{max}{}^{A}$ ($M^{-1}\cdot cm^{-1}$)	$\lambda_{max}{}^{A}$ (nm)	$\varepsilon_{max}{}^{A}$ ($M^{-1}\cdot cm^{-1}$)
12	495	23300	484	28000	501	35300	486	27900	480	33100	491	30900
20	499	35800	496	43700	517	51500	501	35300	496	45500	503	36100
24	503	67500	496	44400	509	81500	496	35900	490	57000	499	5500[a]

[a] Low solubility.

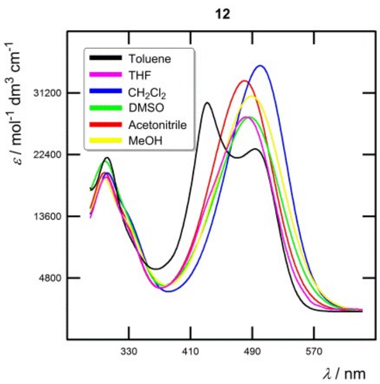

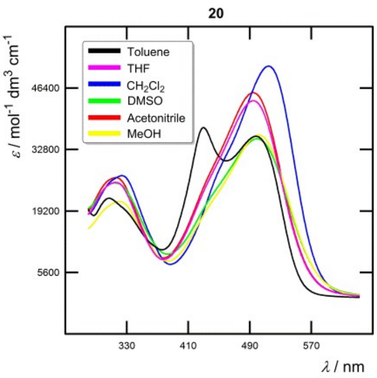

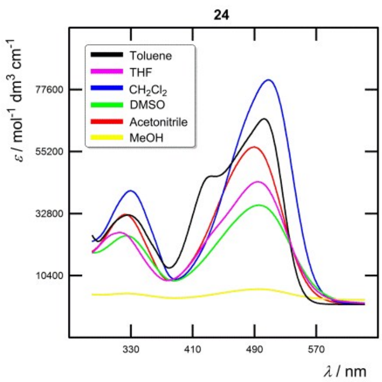

5. Differential scanning calorimetry

Thermal properties of linear, quadrupolar and tripodal chromophores **1-24** were investigated by DSC measurements.

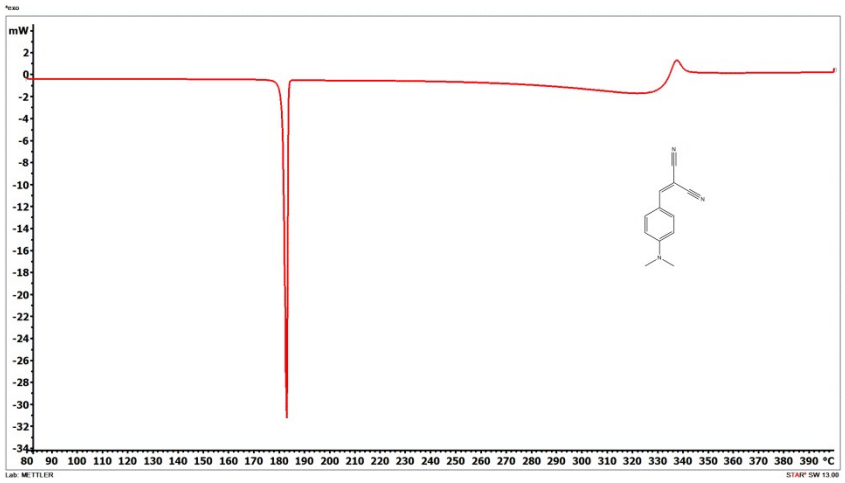

Figure S10. DSC curve of chromophore **1**.

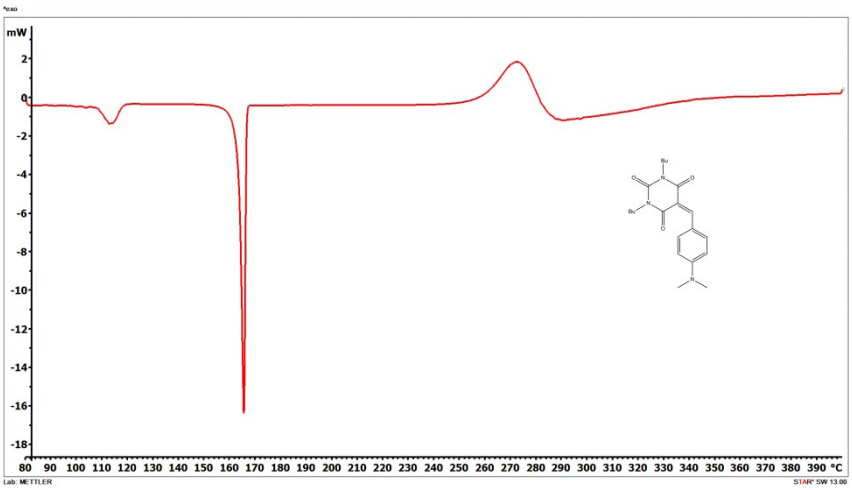

Figure S11. DSC curve of chromophore **2.**

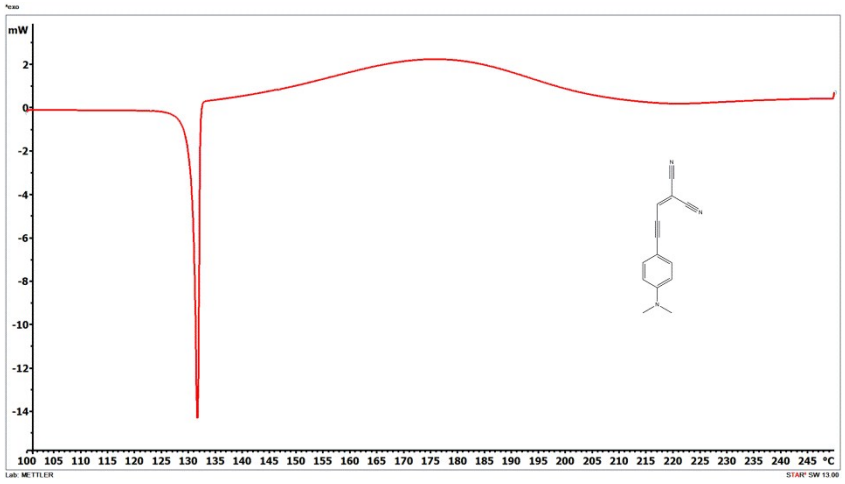

Figure S12. DSC curve of chromophore **3.**

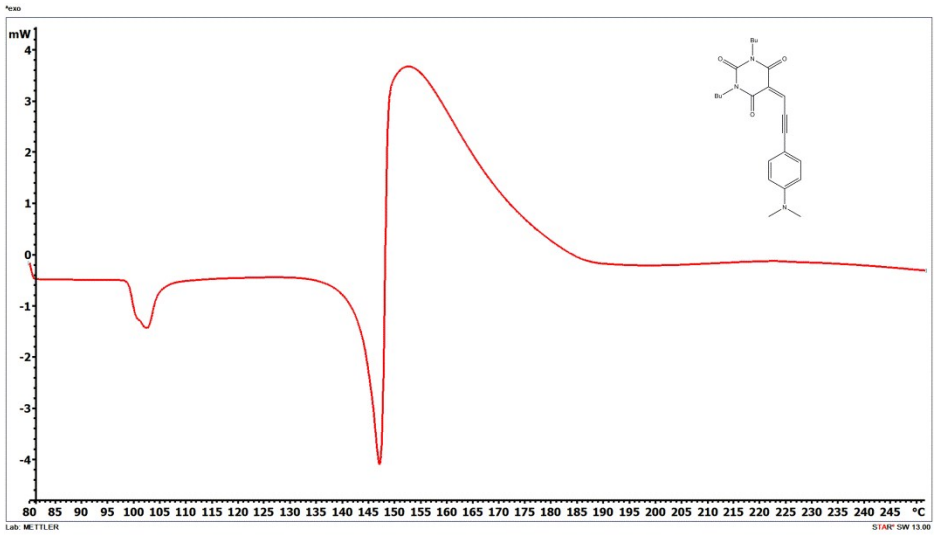

Figure S13. DSC curve of chromophore **4.**

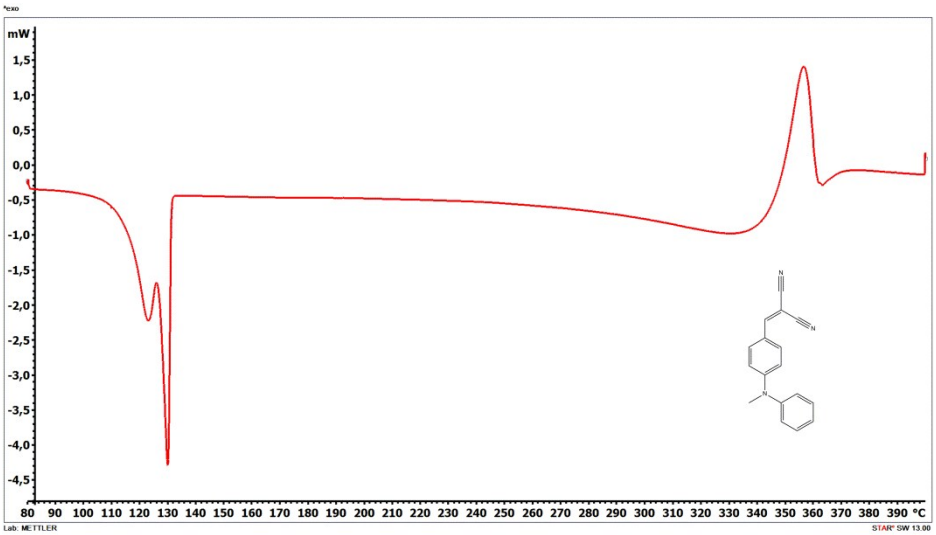

Figure S14. DSC curve of chromophore **5**.

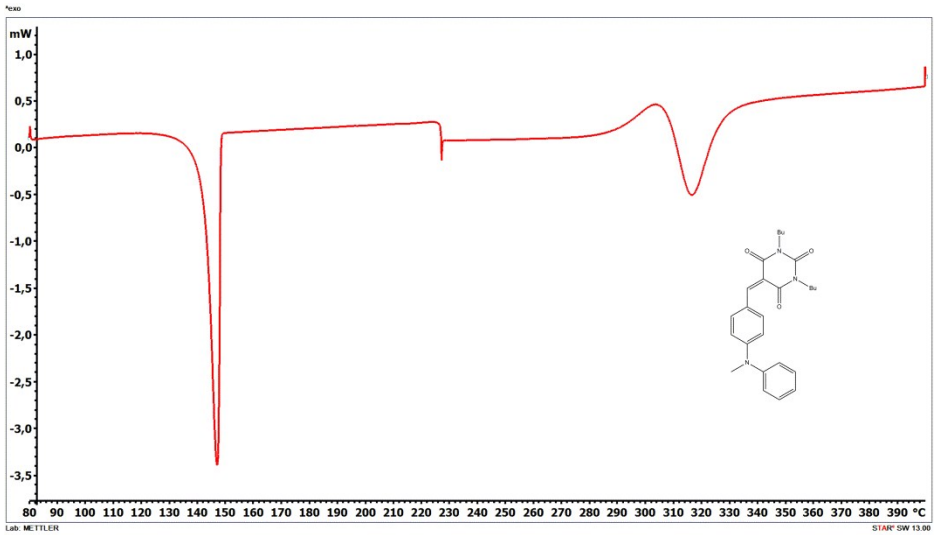

Figure S15. DSC curve of chromophore **6.**

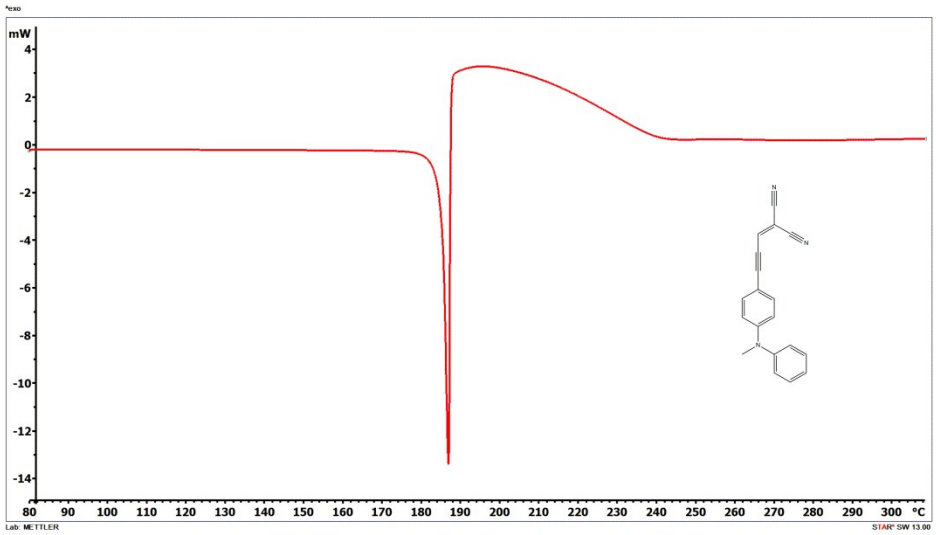

Figure S16. DSC curve of chromophore **7.**

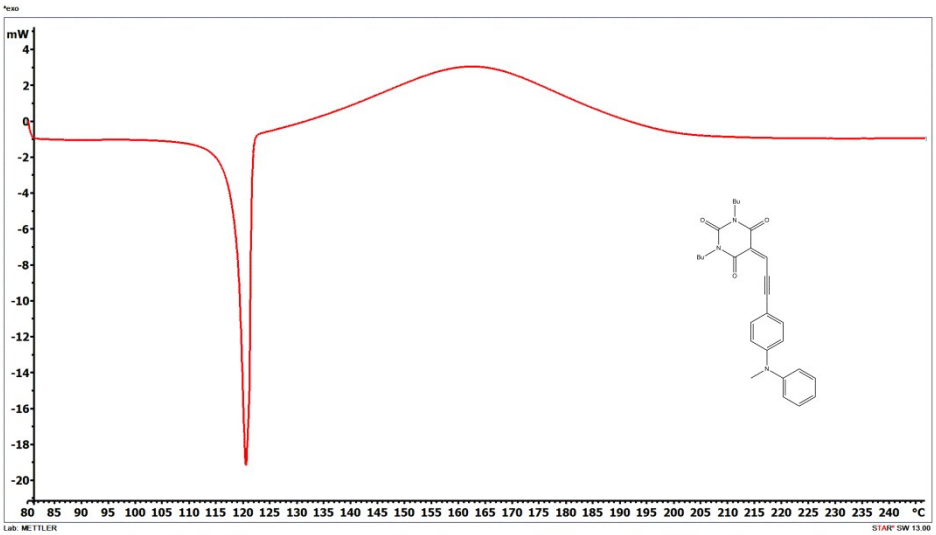

Figure S17. DSC curve of chromophore **8.**

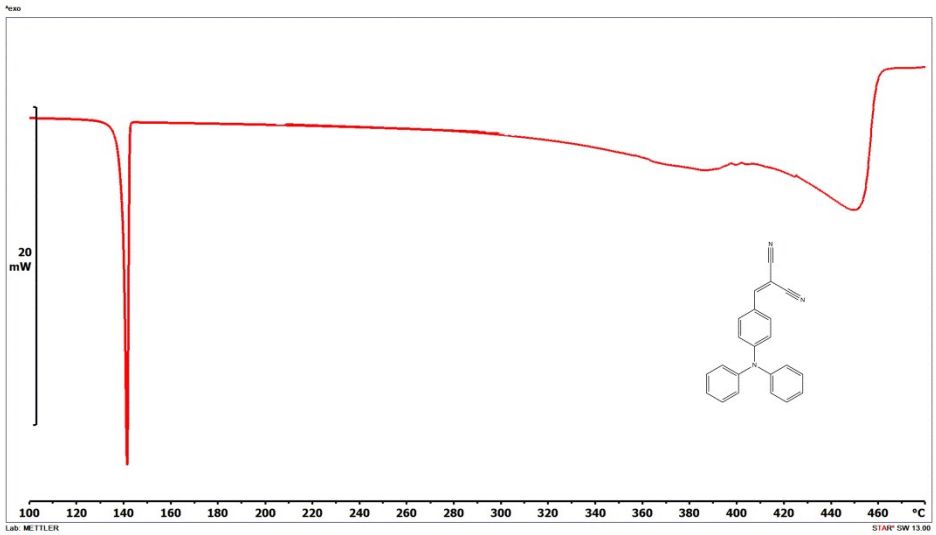

Figure S18. DSC curve of chromophore **9.**

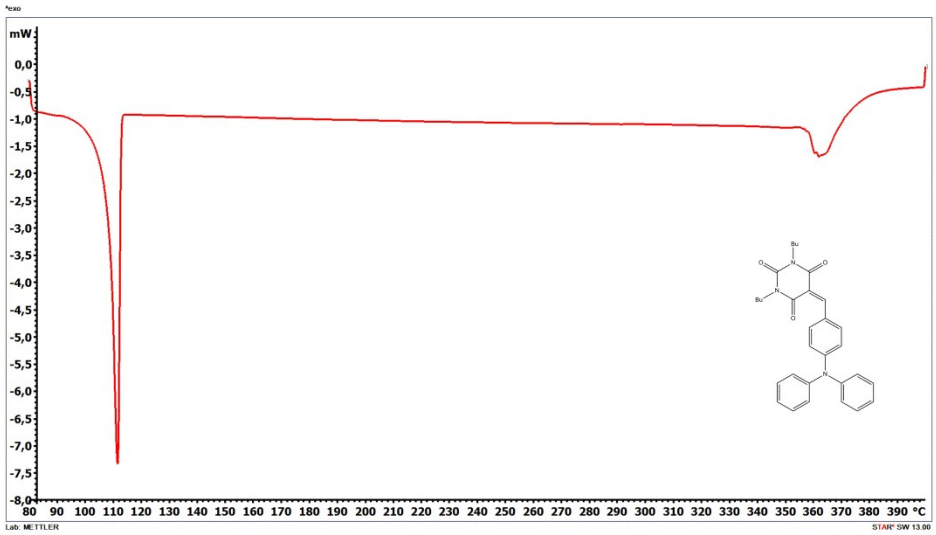

Figure S19. DSC curve of chromophore **10.**

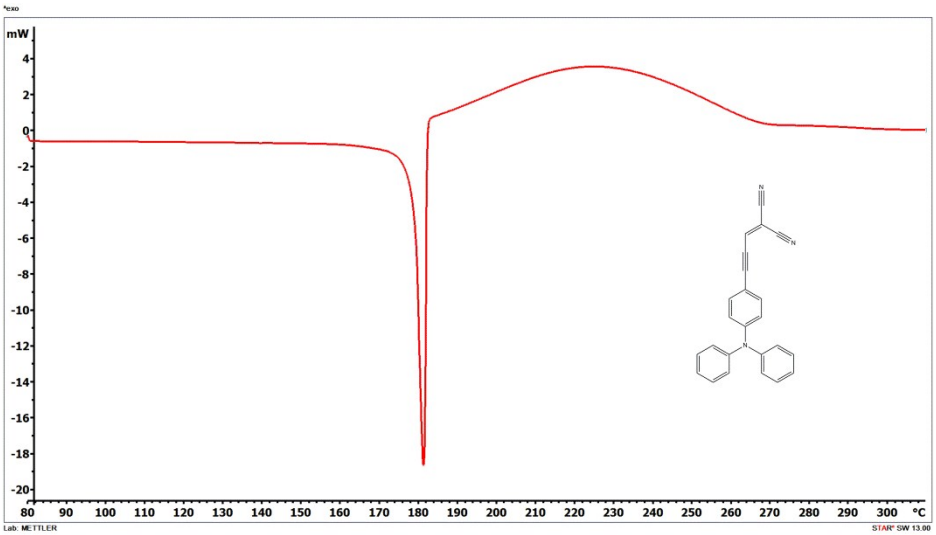

Figure S20. DSC curve of chromophore **11.**

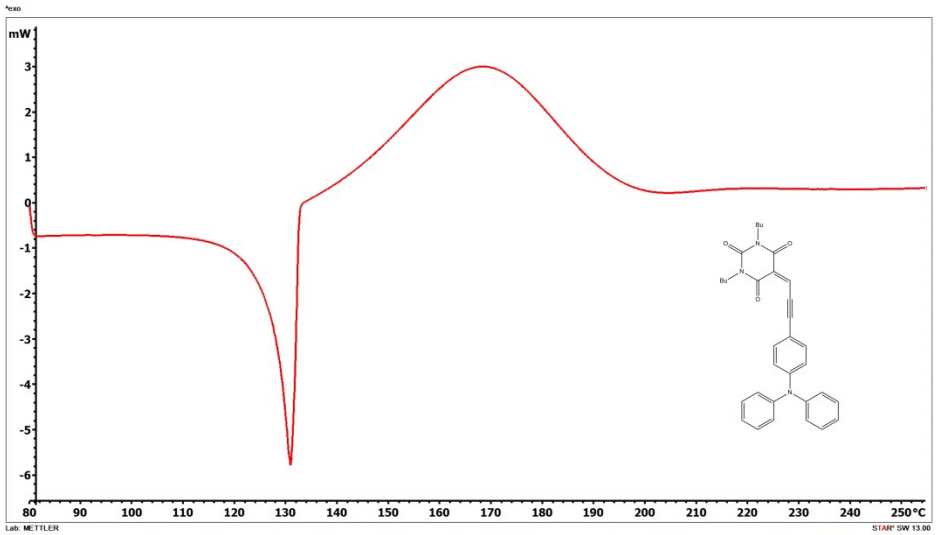

Figure S21. DSC curve of chromophore **12.**

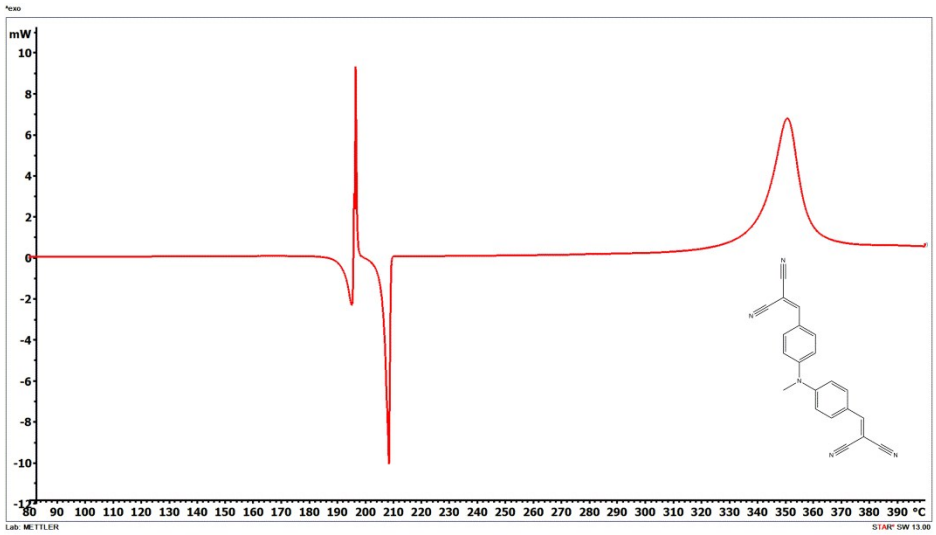

Figure S22. DSC curve of chromophore **13.**

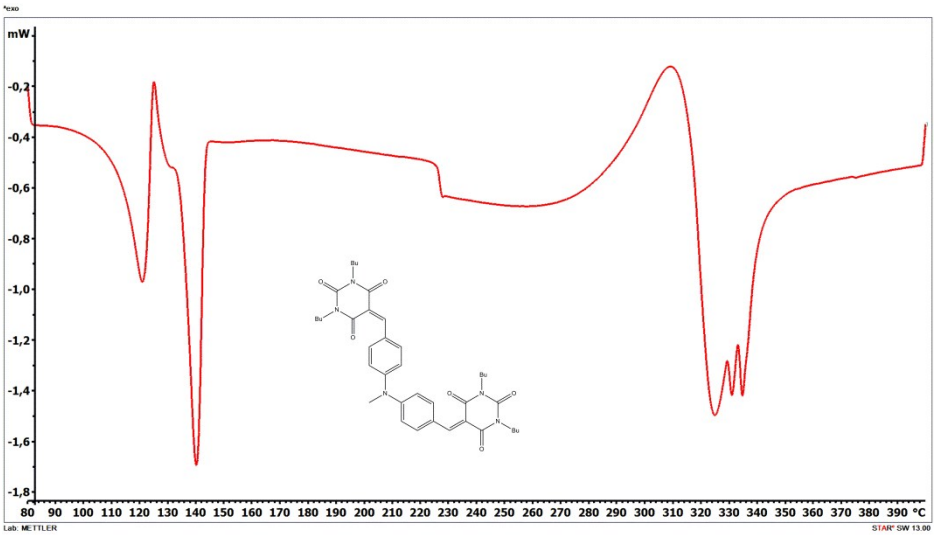

Figure S23. DSC curve of chromophore **14.**

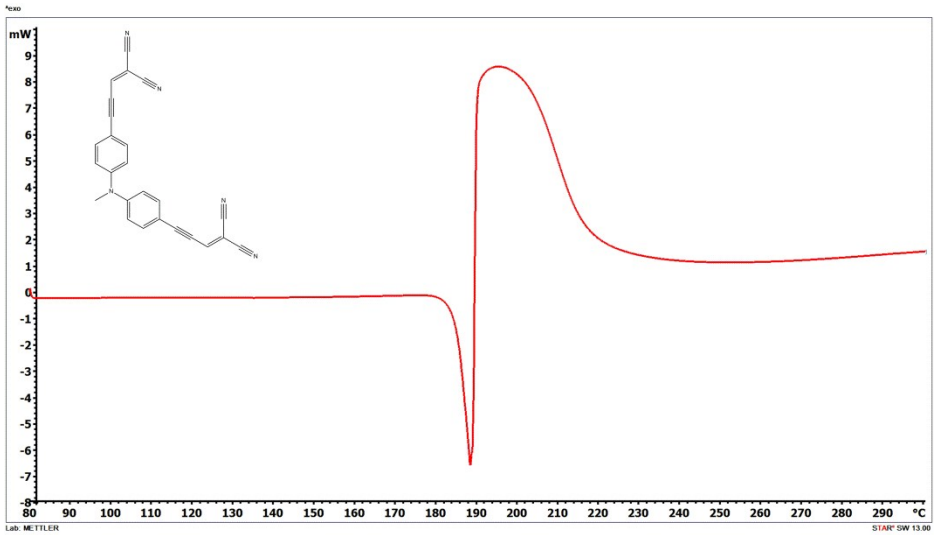

Figure S24. DSC curve of chromophore **15.**

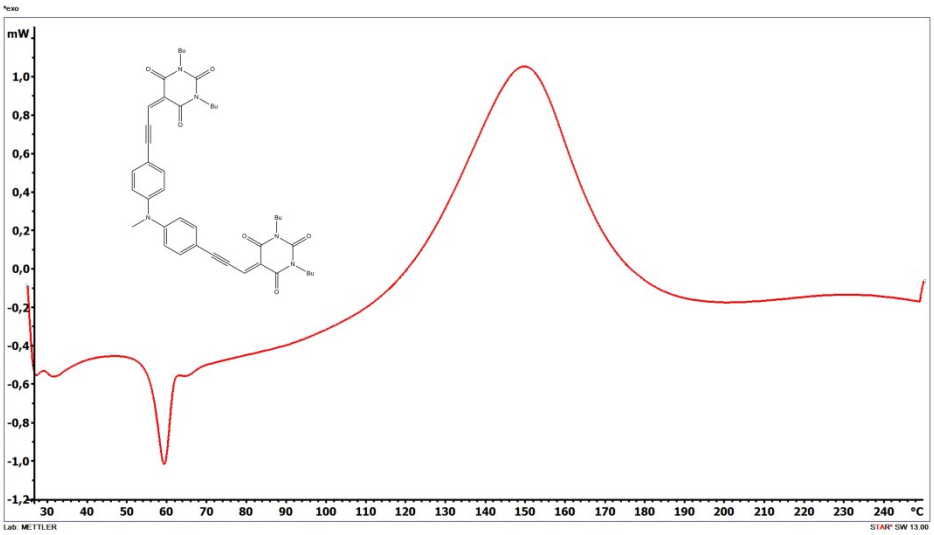

Figure S25. DSC curve of chromophore **16.**

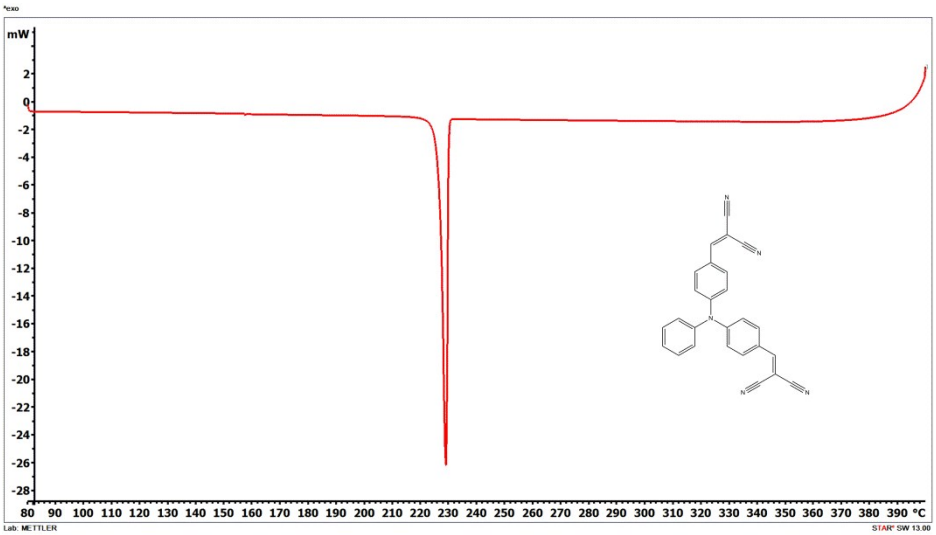

Figure S26. DSC curve of chromophore **17.**

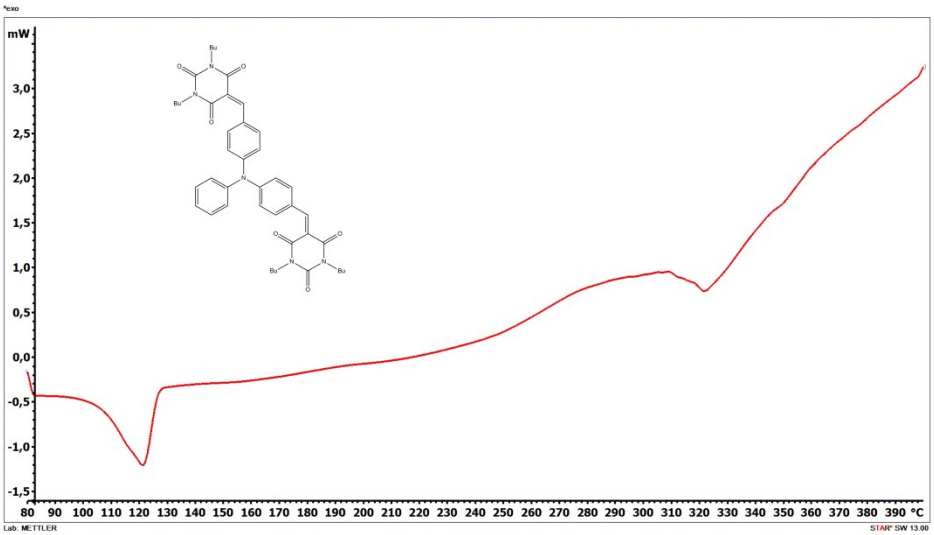

Figure S27. DSC curve of chromophore **18.**

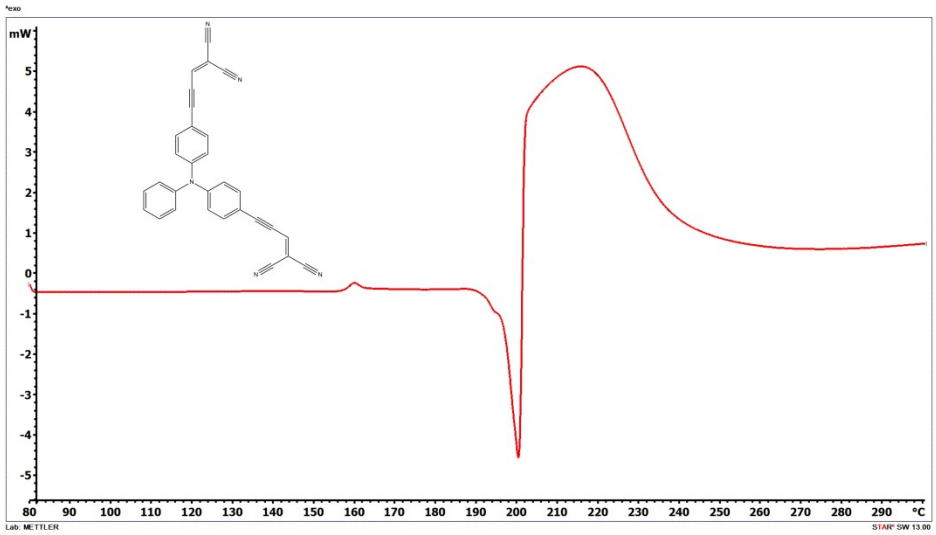

Figure S28. DSC curve of chromophore **19.**

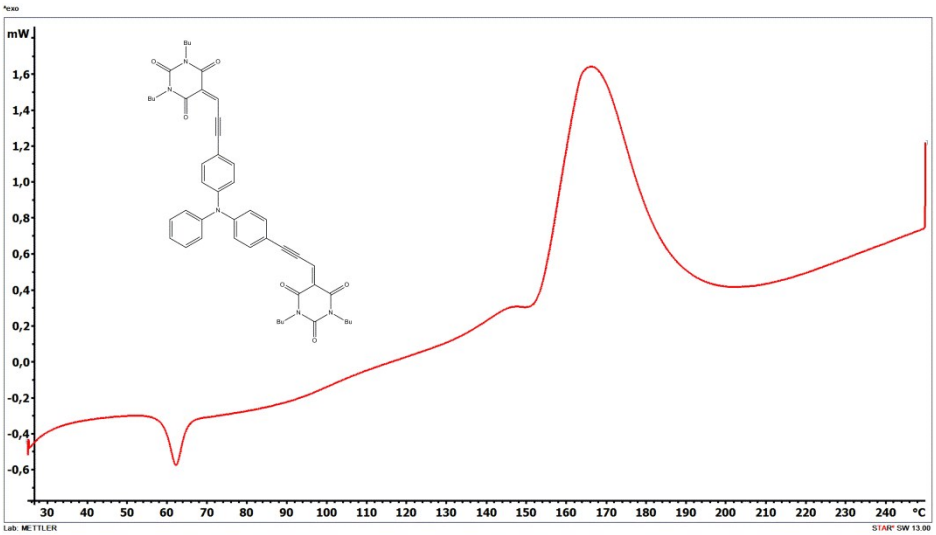

Figure S29. DSC curve of chromophore **20.**

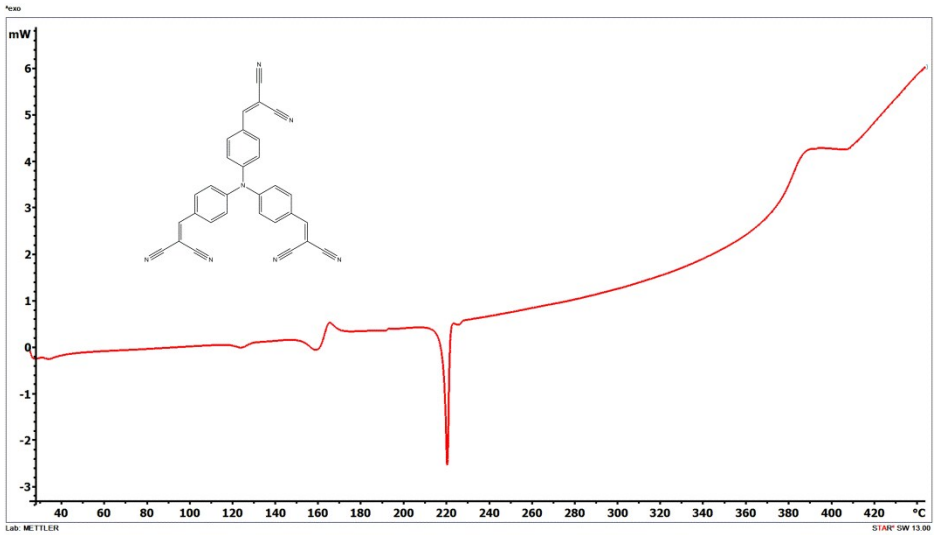

Figure S30. DSC curve of chromophore **21.**

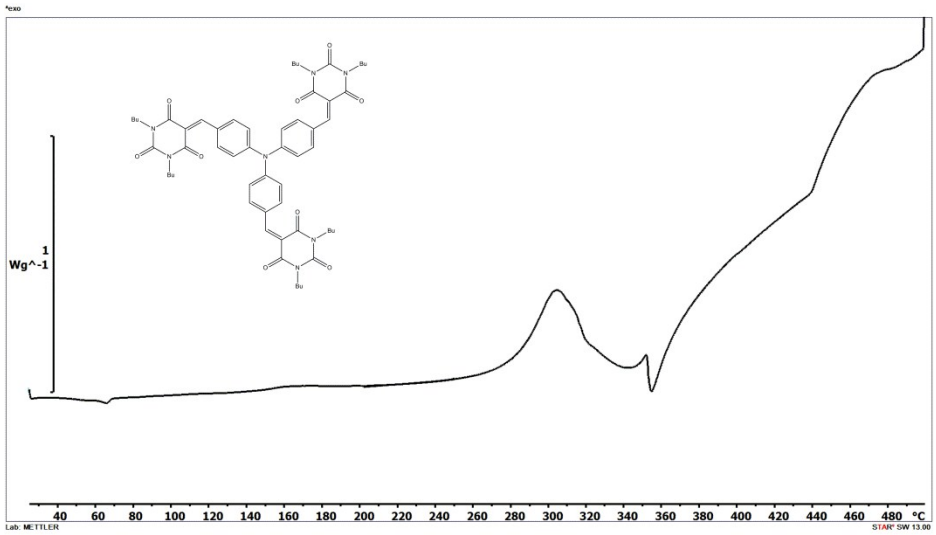

Figure S31. DSC curve of chromophore **22.**

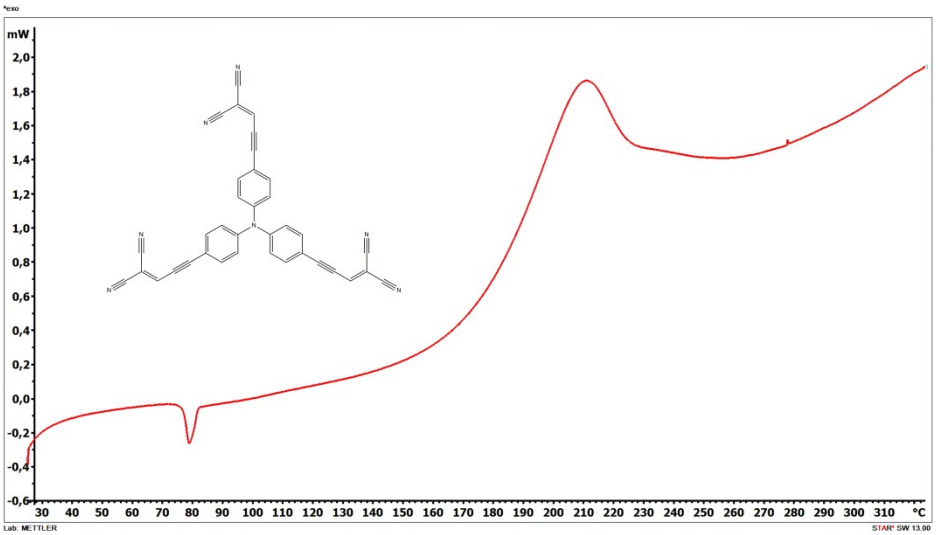

Figure S32. DSC curve of chromophore **23.**

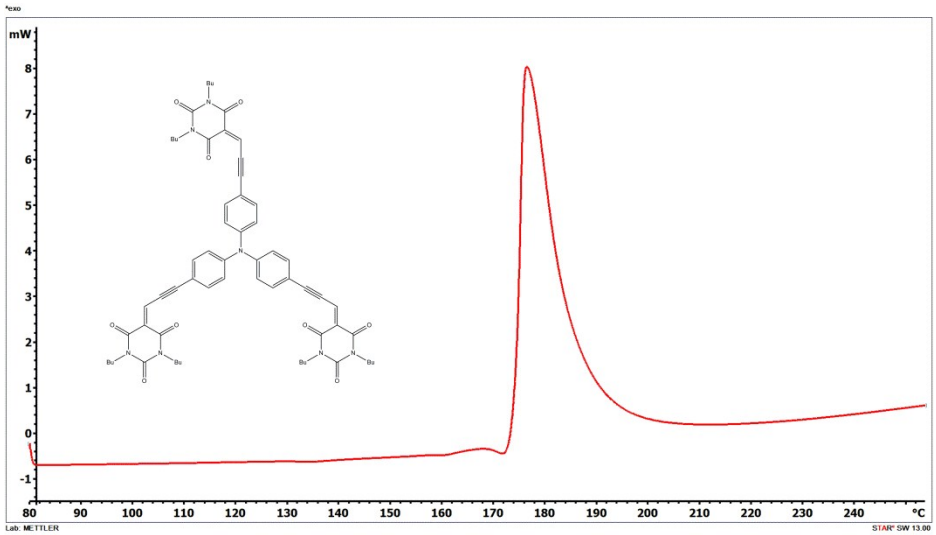

Figure S33. DSC curve of chromophore **24.**

6. DFT calculations

All calculations were carried out in Gaussian 09W (Ref. 12) package at the DFT level of theory. Initial geometry optimizations of chromophores **1-24** were carried out by PM3 method implemented in program ArgusLab (Ref. 13) and subsequently by DFT B3LYP method with 6-311G++(2d,p) basic set. Energies of the HOMO and LUMO (E_{HOMO} and E_{LUMO}), their differences (ΔE) and ground state dipole moments (μ) were calculated by DFT method B3LYP/6-311++G(2d,p). The first hyperpolarizabilities were deducted from the optimized geometries using PM7 method implemented in MOPAC2012 software.[14]

6.1. HOMO/LUMO localizations

The following HOMO and LUMO localizations in molecules **1-24** were derived from the calculations using PM7 method implemented in MOPAC2012 program.[14] Chromophores **16**, **18**, **20**, **22**, **24** were calculated with *N,N´*-dimethylbarbituric moiety due to acceleration of calculations and almost zero influence of butyl substituents on the electron density distribution along the molecule.The visualizations have been performed in program OPchem.[15]

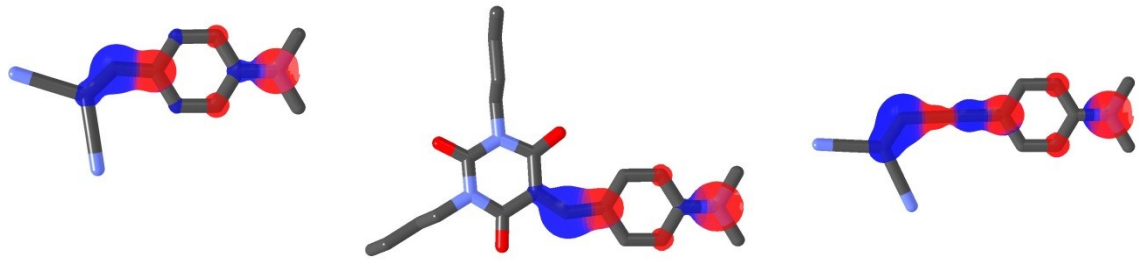

Figure S34. HOMO (red) and LUMO (blue) localizations in linear chromophores **1-3.**

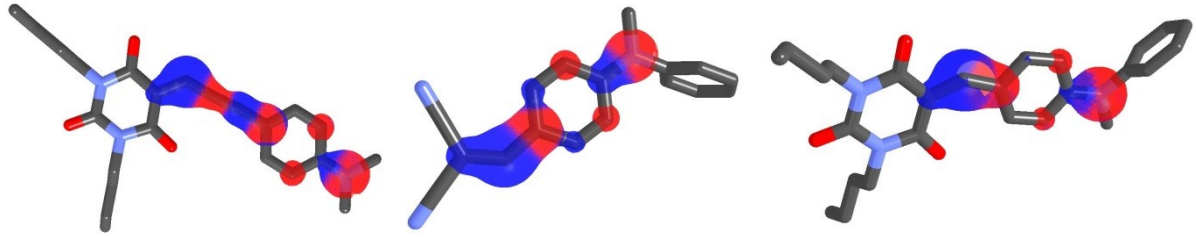

Figure S35. HOMO (red) and LUMO (blue) localizations in linear chromophores **4-6**.

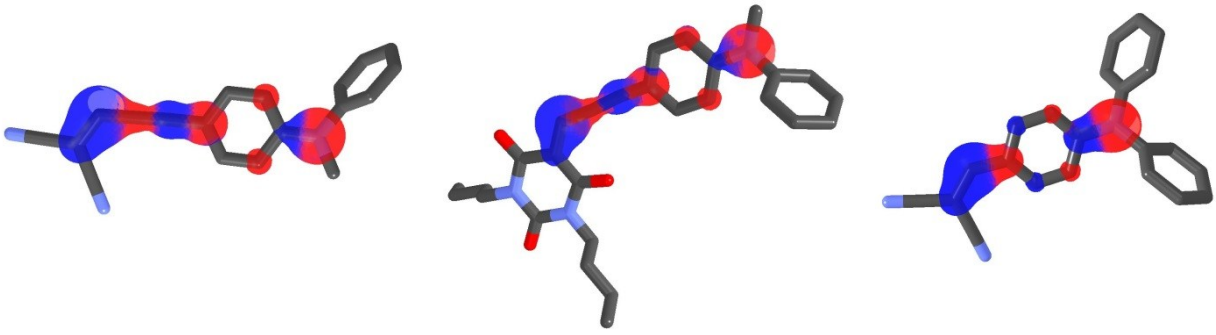

Figure S36. HOMO (red) and LUMO (blue) localizations in linear chromophores **7-9.**

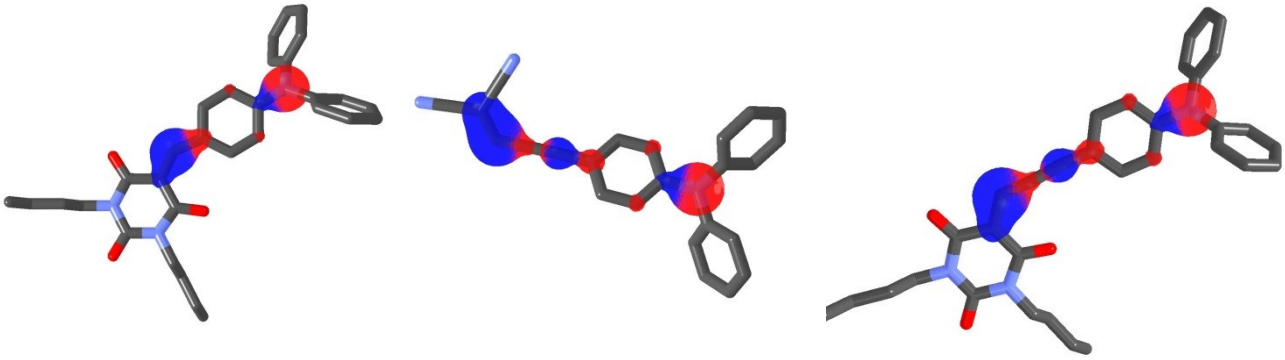

Figure S37. HOMO (red) and LUMO (blue) localizations in linear chromophores **10-12.**

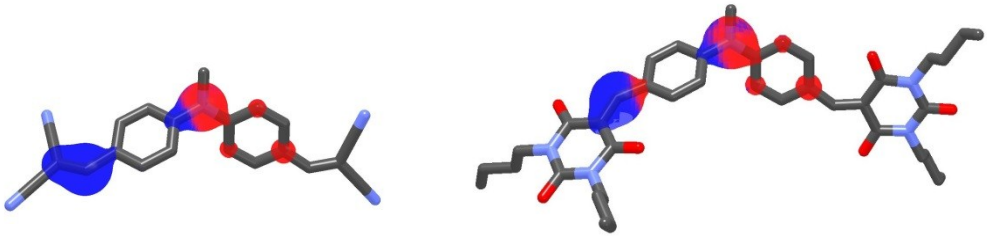

Figure S38. HOMO (red) and LUMO (blue) localizations in quadrupolar chromophores **13-14.**

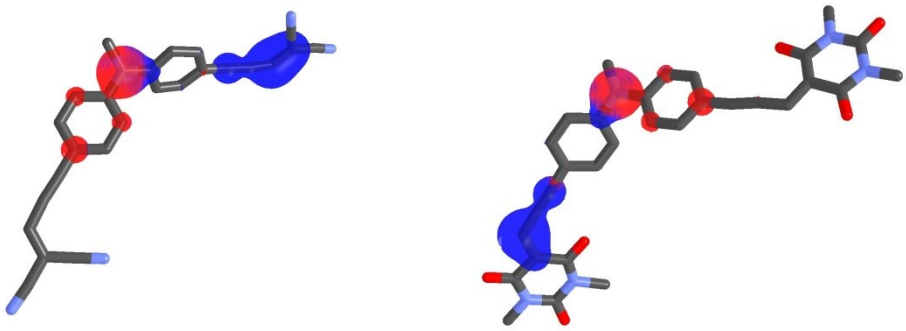

Figure S39. HOMO (red) and LUMO (blue) localizations in quadrupolar chromophores **15-16.**

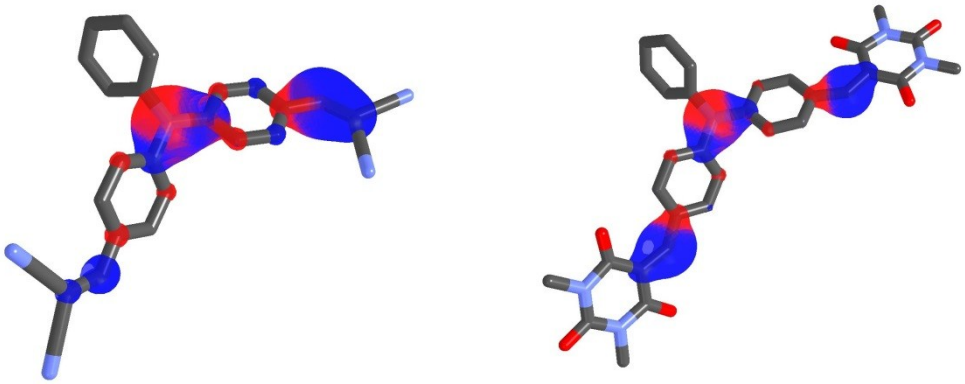

Figure S40. HOMO (red) and LUMO (blue) localizations in quadrupolar chromophores **17-18.**

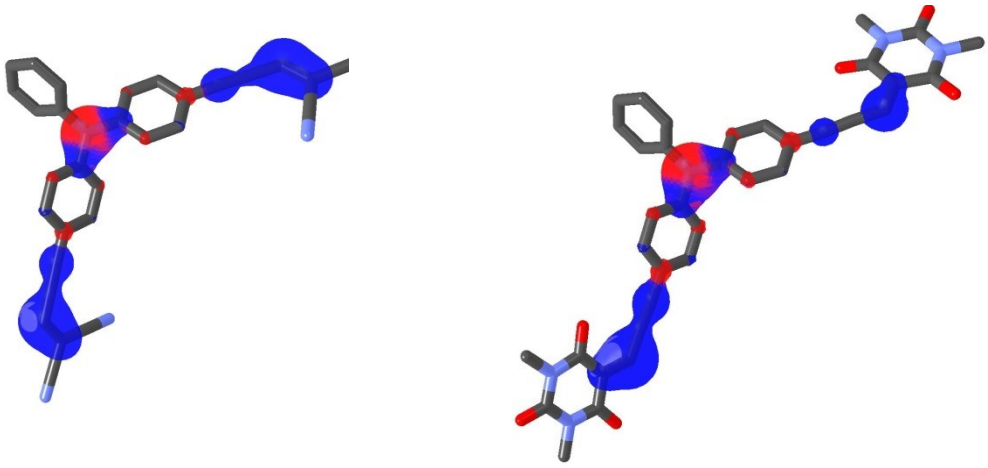

Figure S41. HOMO (red) and LUMO (blue) localizations in quadrupolar chromophores **19-20.**

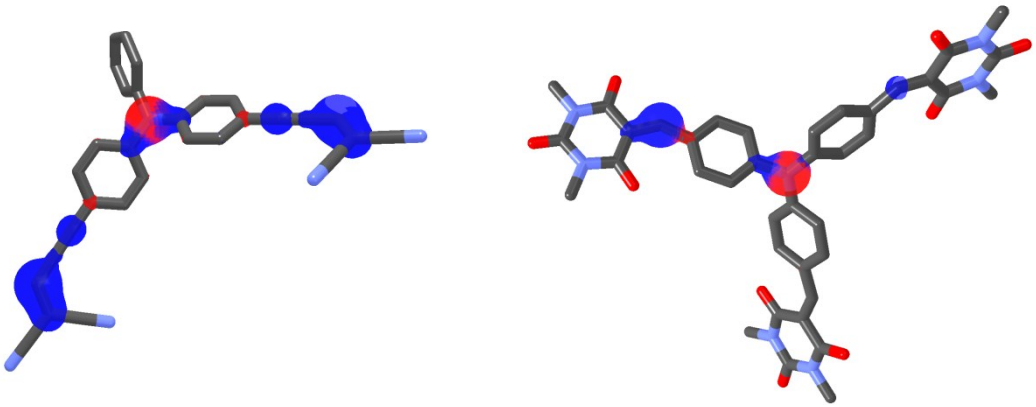

Figure S42. HOMO (red) and LUMO (blue) localizations in tripodal chromophores **21-22.**

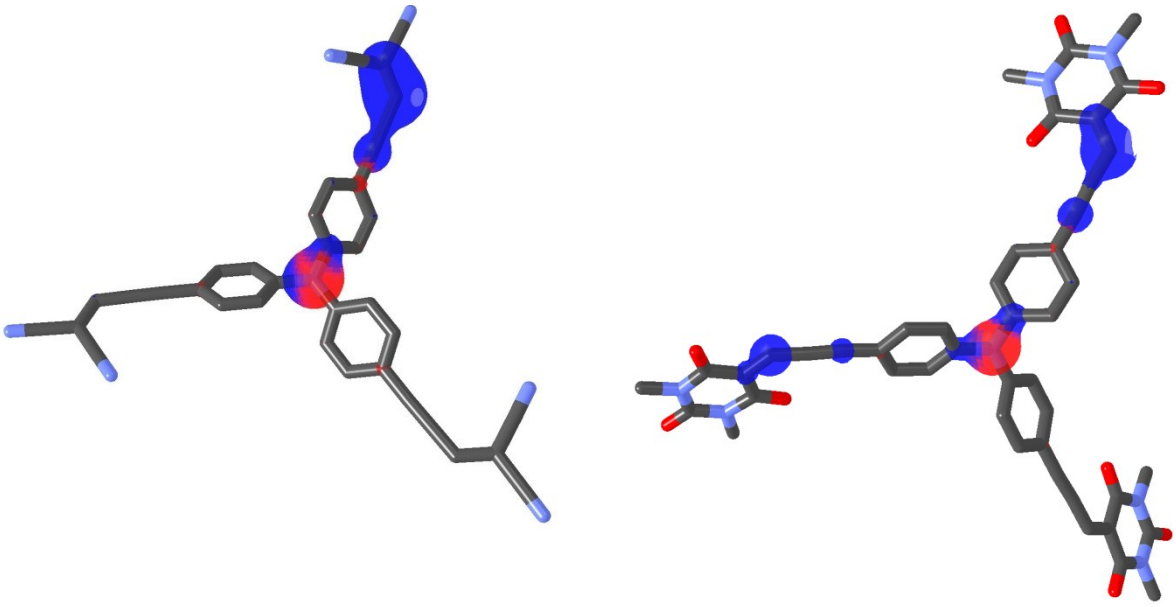

Figure S43. HOMO (red) and LUMO (blue) localizations in tripodal chromophores **23-24.**

7. Correlations

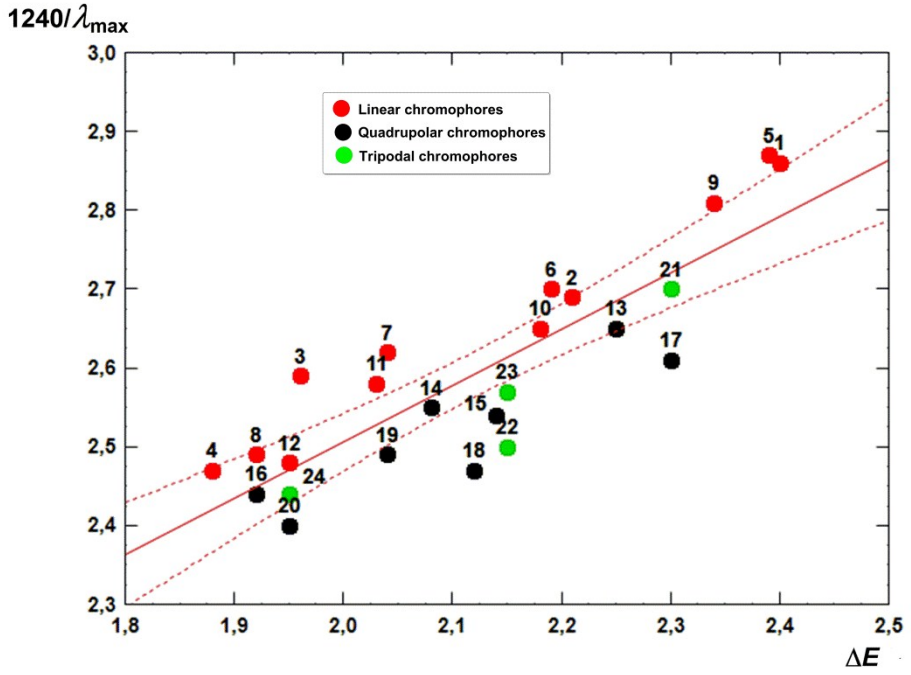

Figure S44. Correlation of the energy of the longest-wavelenght absorption maxima 1240/λ_{max} and the electrochemical gap ΔE (R = 0.86).

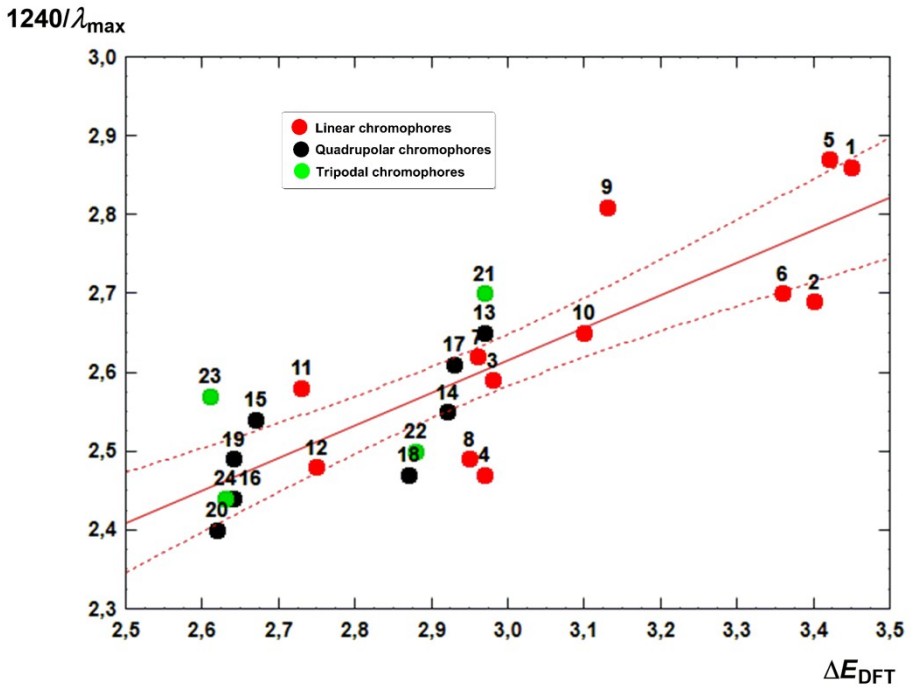

Figure S45. Correlation of the energy of the longest-wavelenght absorption maxima 1240/λ_{max} and the calculated electrochemical gap ΔE (R = 0.83).

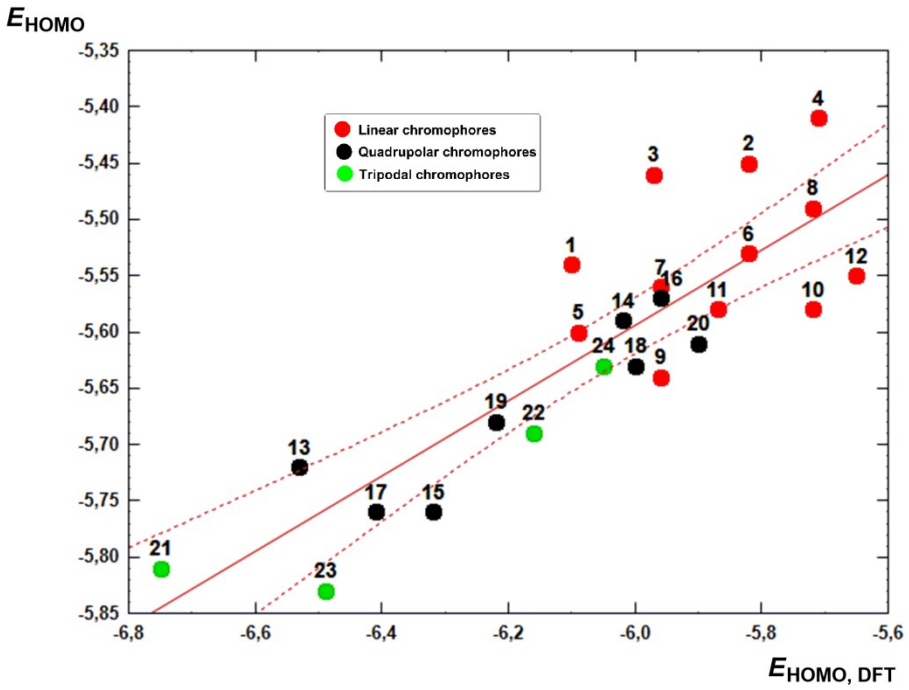

Figure S46. Correlation of the electrochemically derived HOMO energies (E_{HOMO}) vs. calculated ones ($E_{HOMO,DFT}$) (R = 0.86).

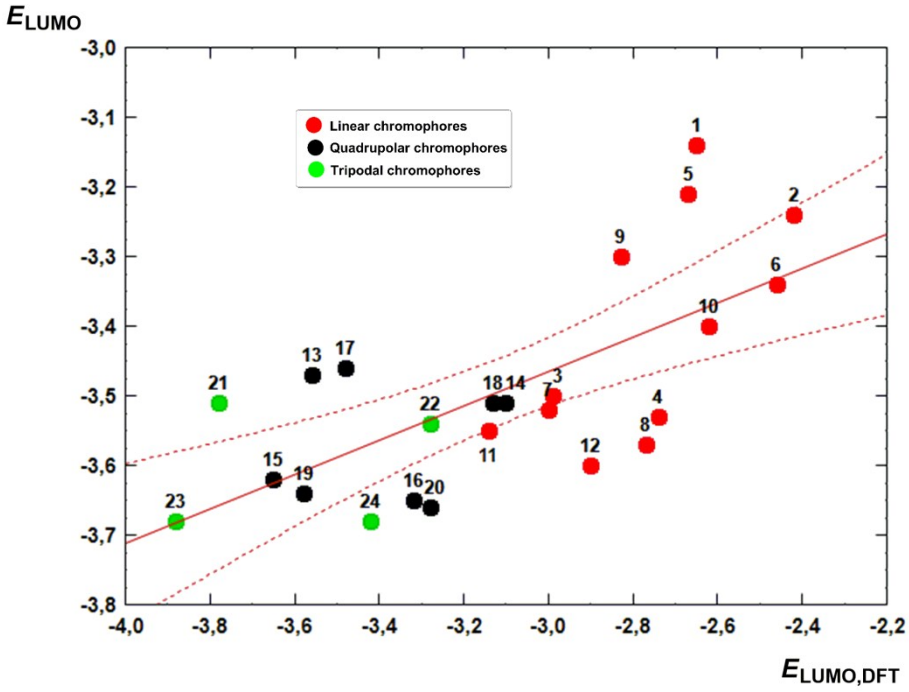

Figure S47. Correlation of the electrochemically derived LUMO energies (E_{LUMO}) vs. calculated ones ($E_{LUMO,DFT}$) (R = 0.68).

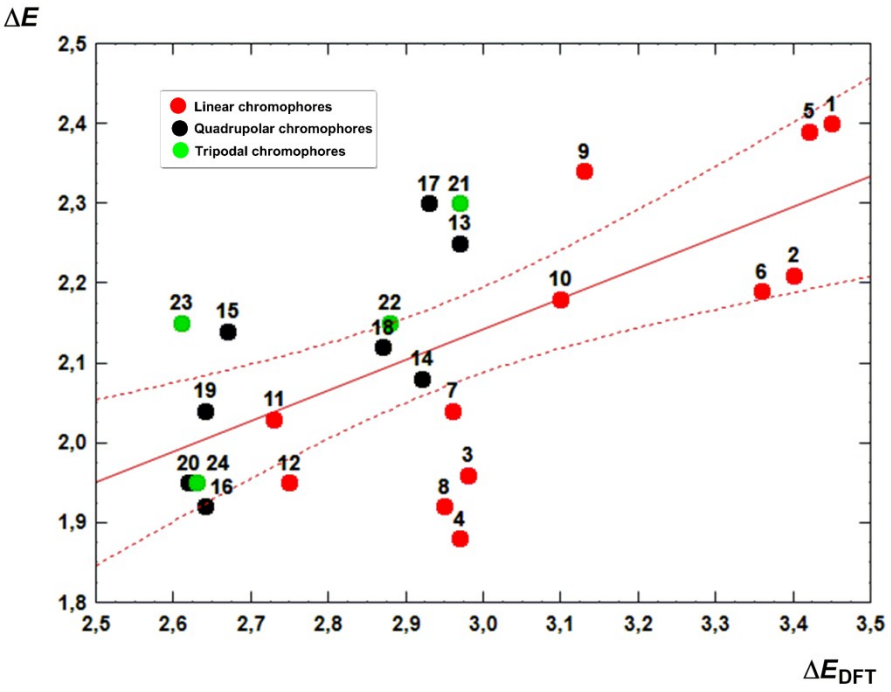

Figure S48. Correlation of the electrochemical gap ΔE and the calculated ones ΔE_{DFT} (R = 0.64).

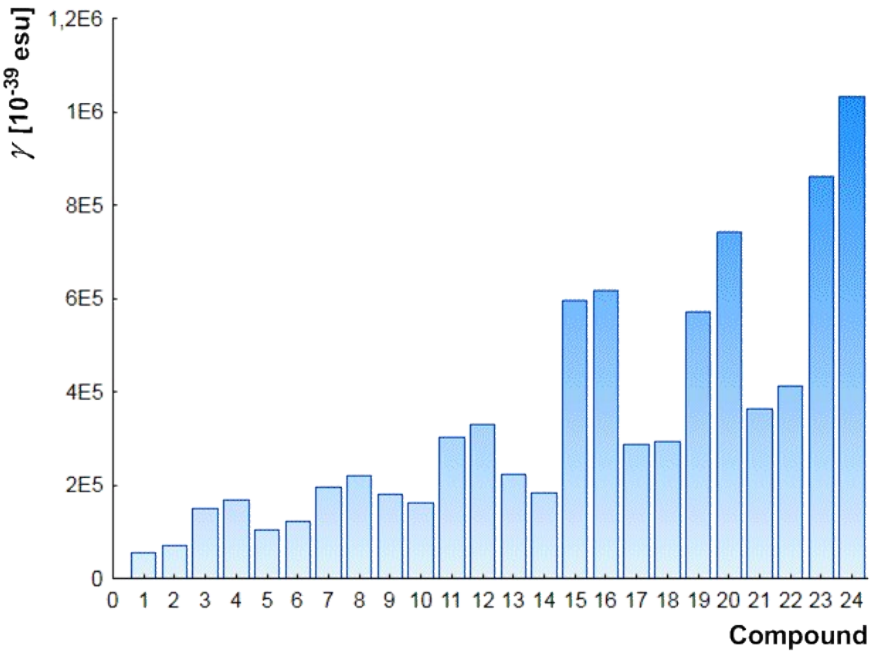

Figure S49. Bar chart of the calculated values for third hyperpolarizability γ.

8. ^{1}H a ^{13}C NMR spectra

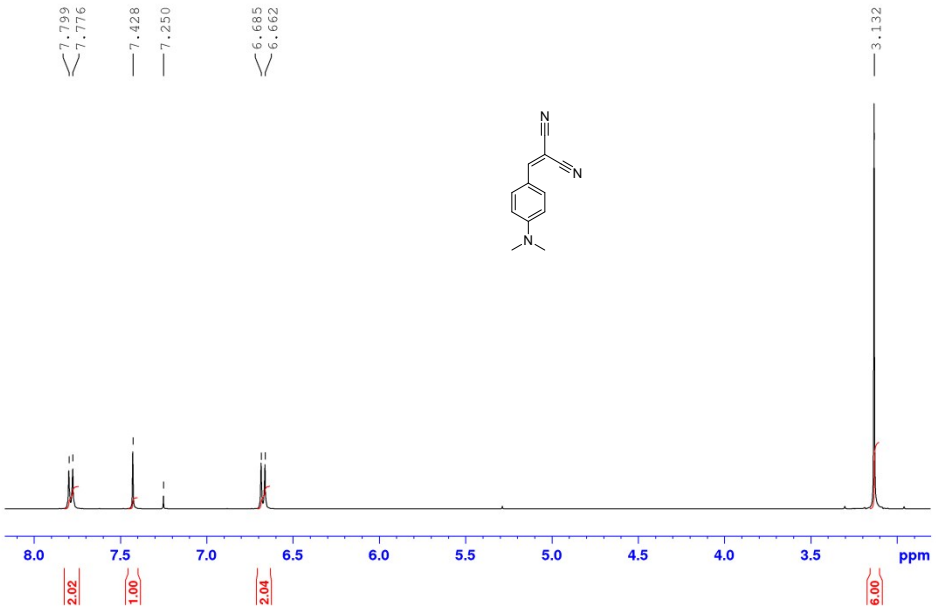

Figure S50. ^{1}H NMR spectrum of chromophore **1** (400 MHz, $CDCl_3$, 25 °C).

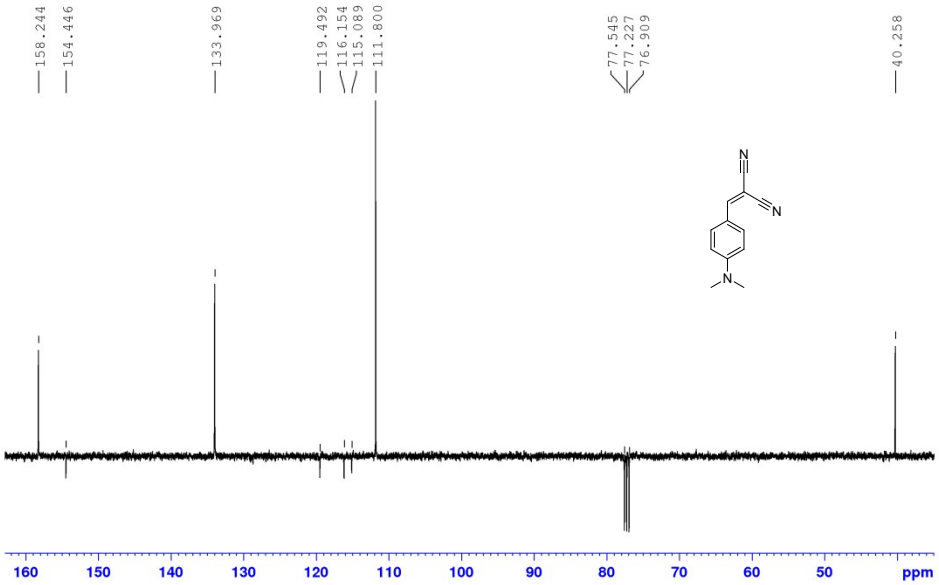

Figure S51. ^{13}C NMR APT spectrum of chromophore **1** (100 MHz, $CDCl_3$, 25 °C).

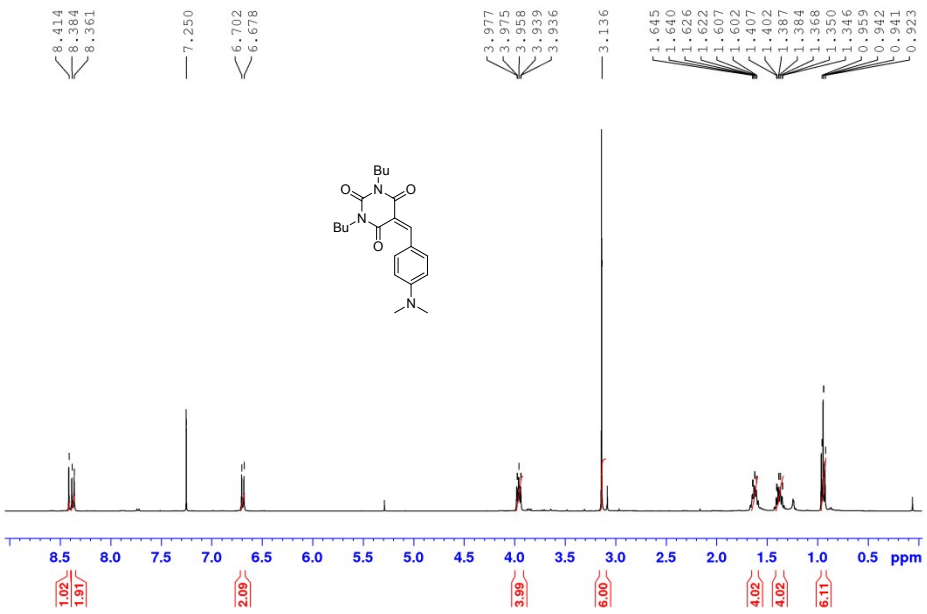

Figure S52. ^{1}H NMR spectrum of chromophore **2** (400 MHz, $CDCl_3$, 25 °C).

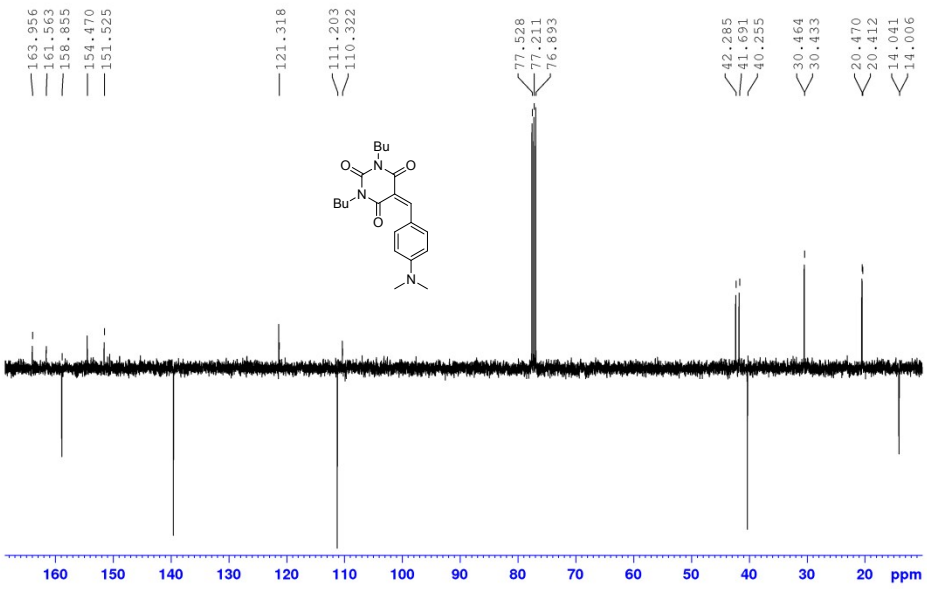

Figure S53. ^{13}C NMR APT spectrum of chromophore **2** (100 MHz, $CDCl_3$, 25 °C).

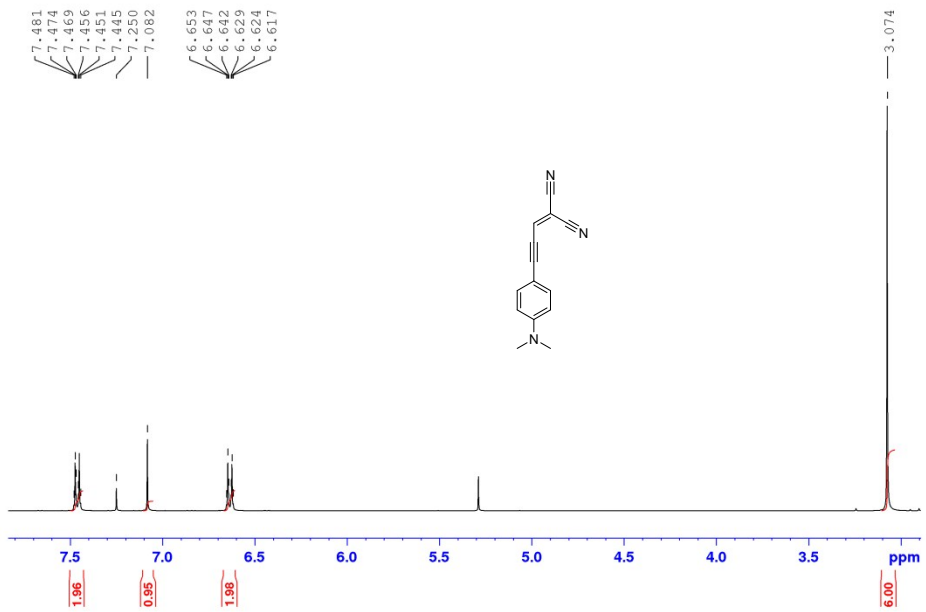

Figure S54. ^{1}H NMR spectrum of chromophore **3** (400 MHz, $CDCl_3$, 25 °C).

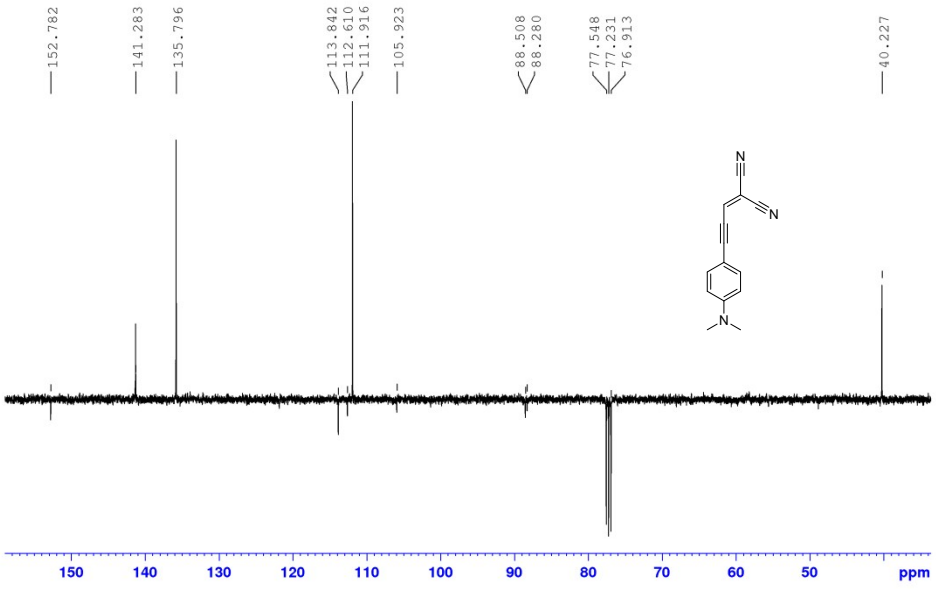

Figure S55. ^{13}C NMR APT spectrum of chromophore **3** (100 MHz, $CDCl_3$, 25 °C).

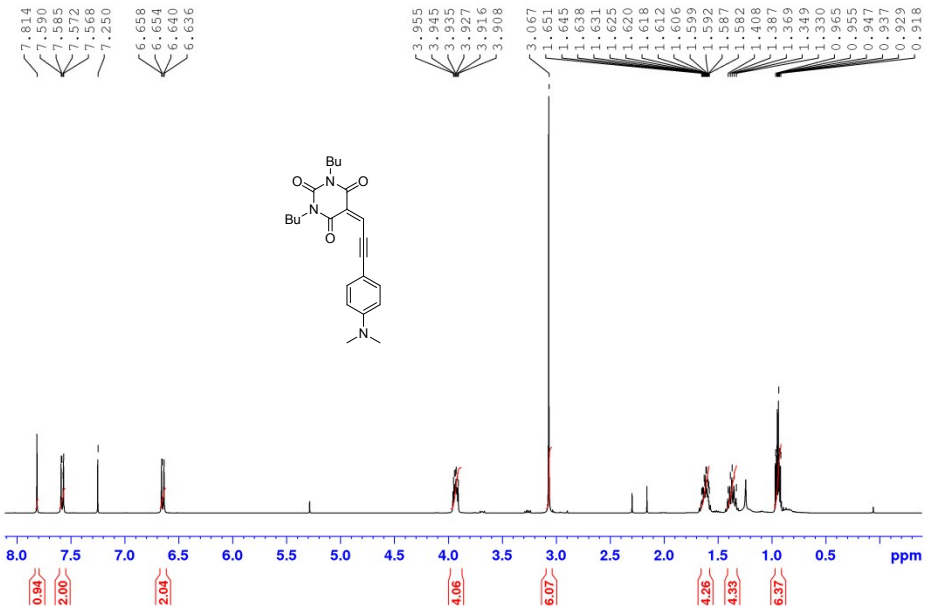

Figure S56. ^{1}H NMR spectrum of chromophore **4** (400 MHz, $CDCl_3$, 25 °C).

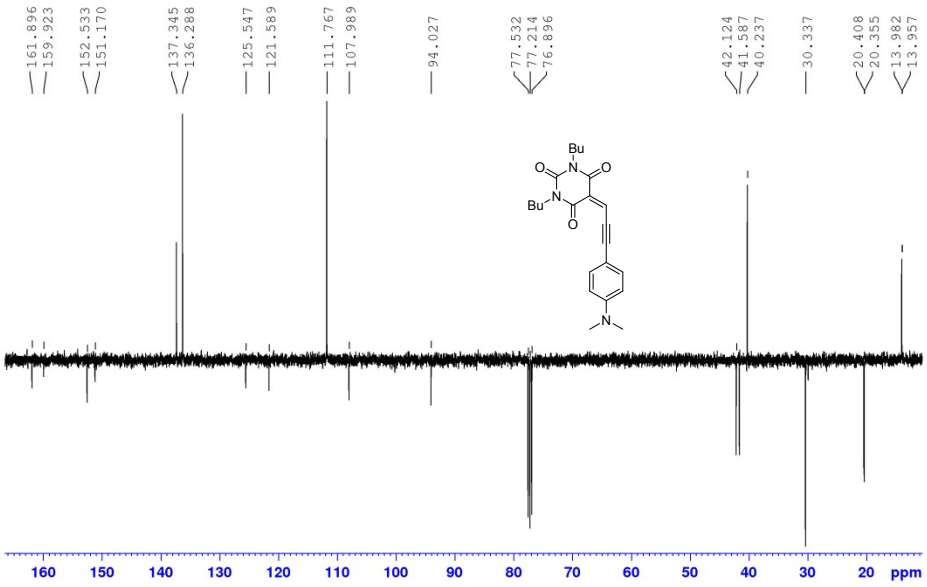

Figure S57. ^{13}C NMR APT spectrum of chromophore **4** (100 MHz, $CDCl_3$, 25 °C).

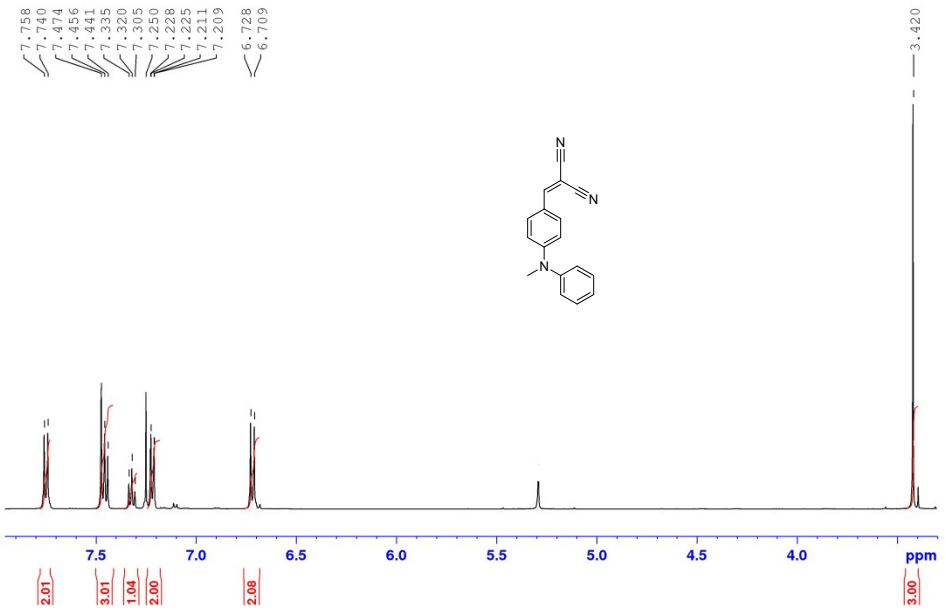

Figure S58. ^{1}H NMR spectrum of chromophore **5** (500 MHz, $CDCl_3$, 25 °C).

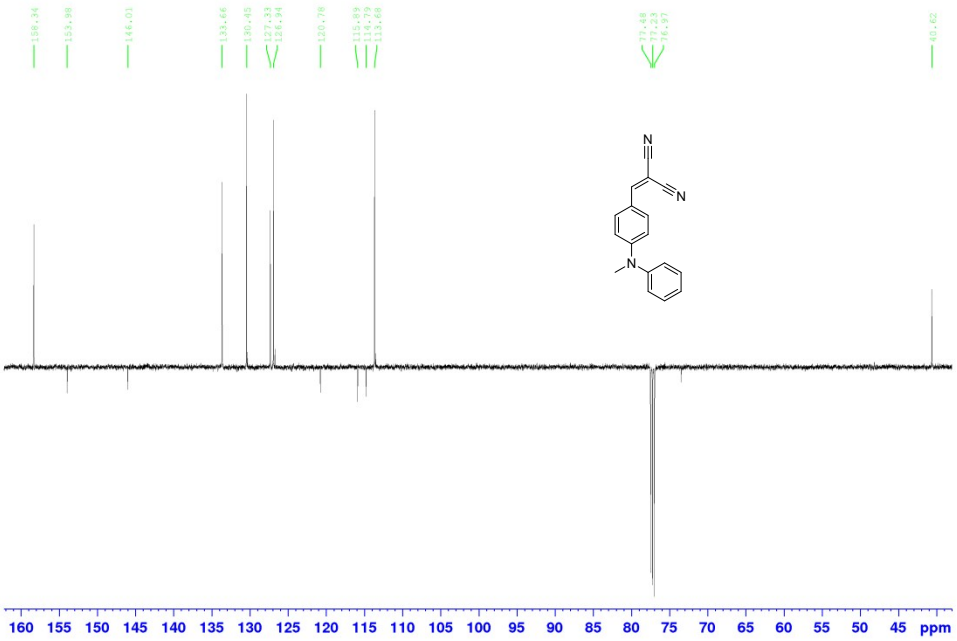

Figure S59. ^{13}C NMR APT spectrum of chromophore **5** (125 MHz, $CDCl_3$, 25 °C).

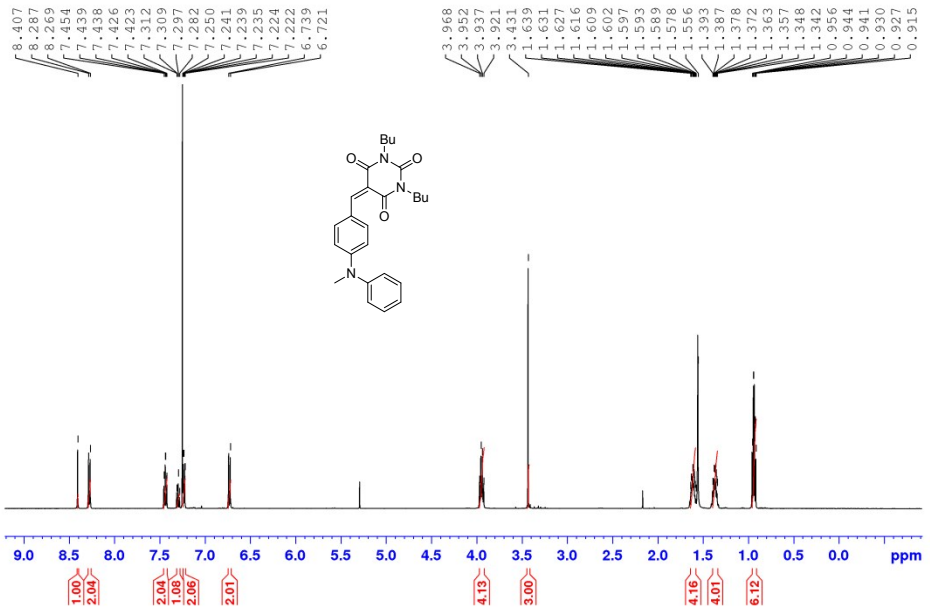

Figure S60. ^{1}H NMR spectrum of chromophore **6** (500 MHz, $CDCl_3$, 25 °C).

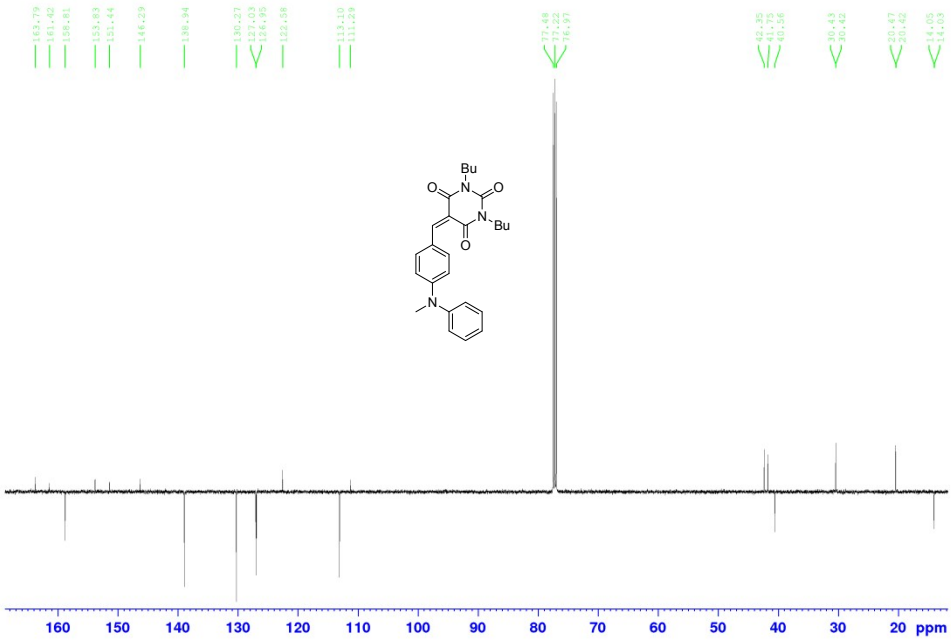

Figure S61. ^{13}C NMR APT spectrum of chromophore **6** (125 MHz, $CDCl_3$, 25 °C).

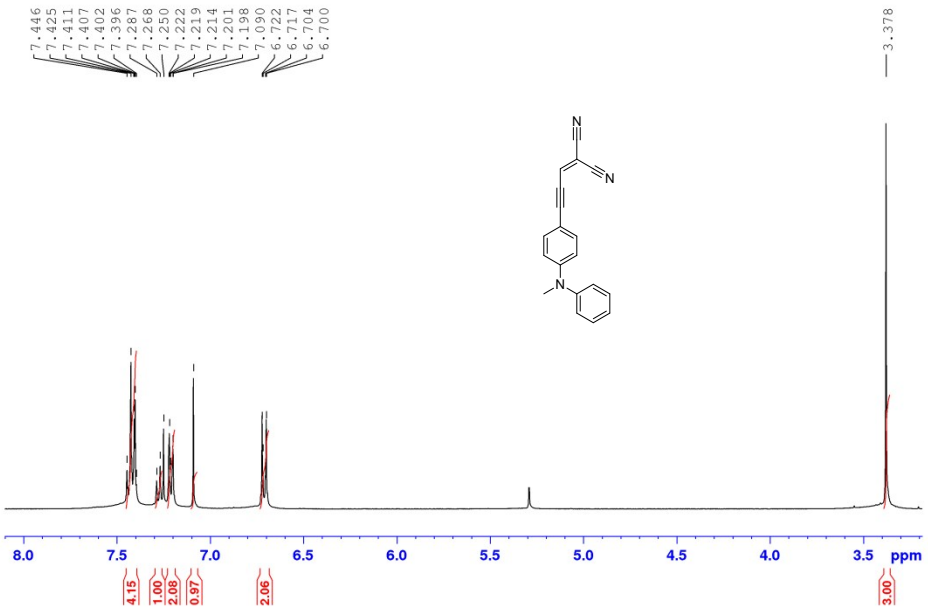

Figure S62. ^{1}H NMR spectrum of chromophore **7** (400 MHz, $CDCl_3$, 25 °C).

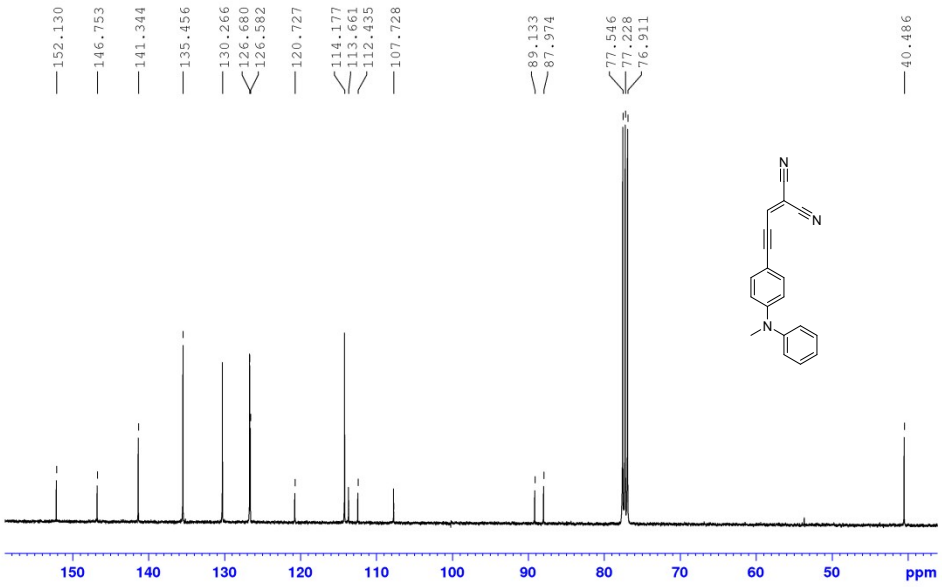

Figure S63. ^{13}C NMR APT spectrum of chromophore **7** (100 MHz, $CDCl_3$, 25 °C).

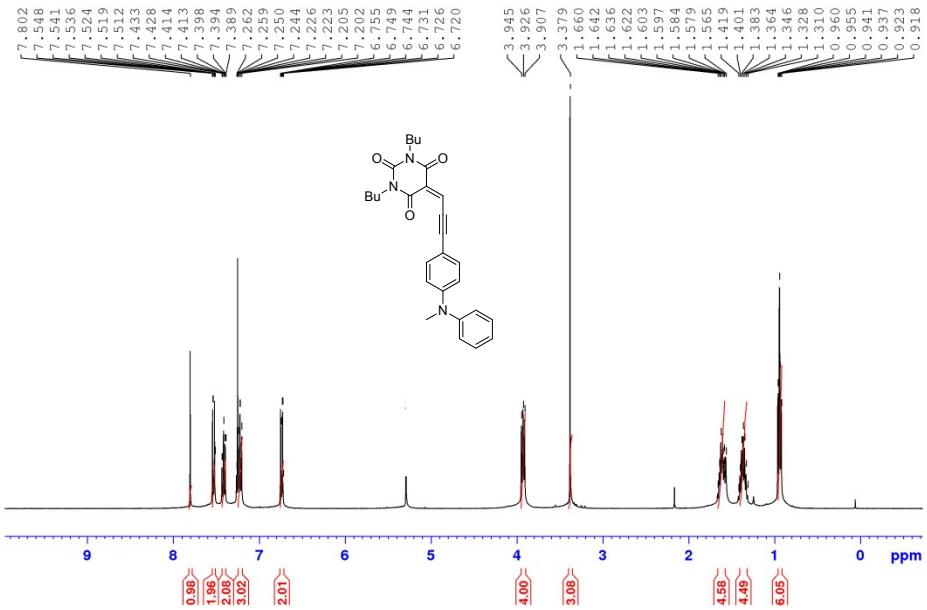

Figure S64. ^{1}H NMR spectrum of chromophore **8** (400 MHz, $CDCl_3$, 25 °C).

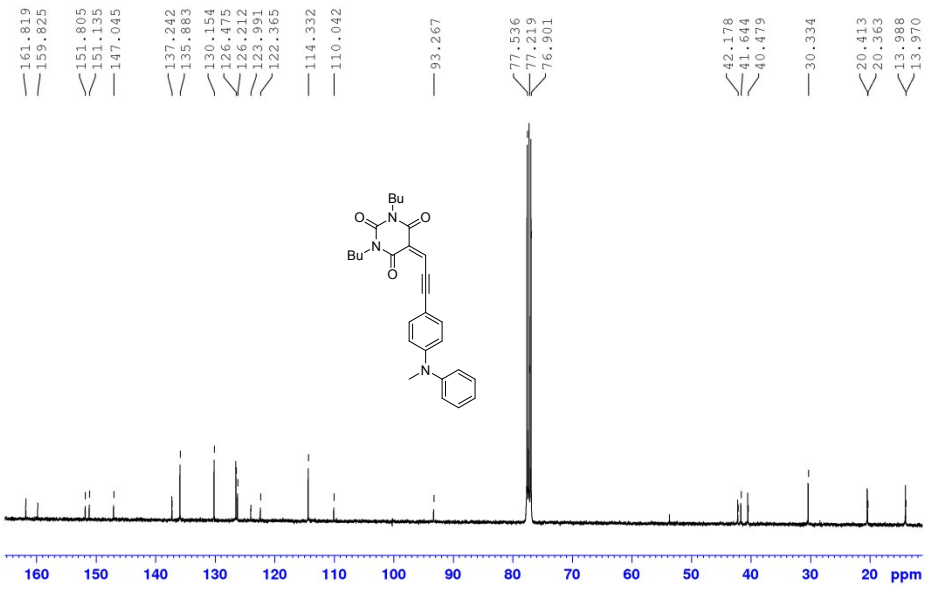

Figure S65. ^{13}C NMR APT spectrum of chromophore **8** (100 MHz, $CDCl_3$, 25 °C).

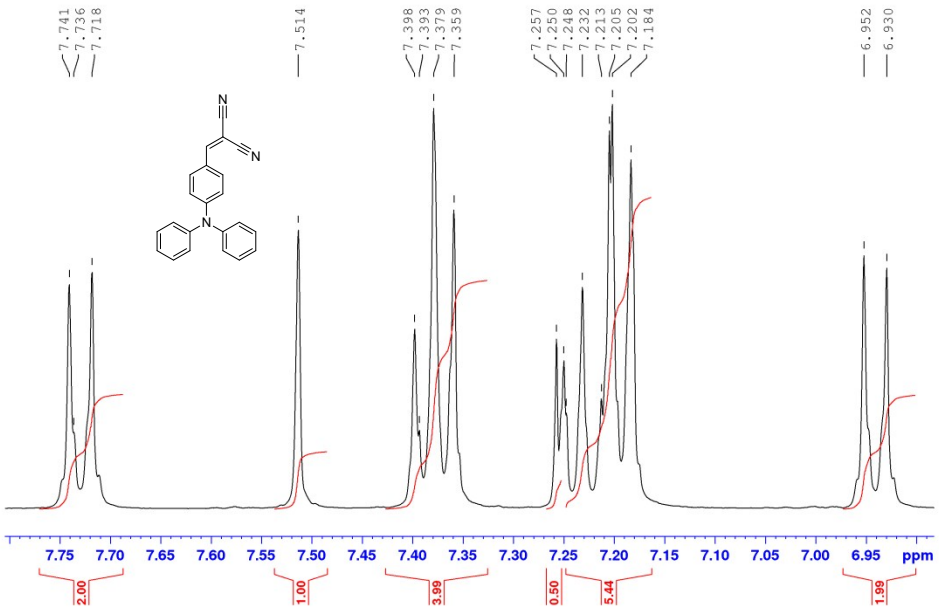

Figure S66. ^{1}H NMR spectrum of chromophore **9** (400 MHz, $CDCl_3$, 25 °C).

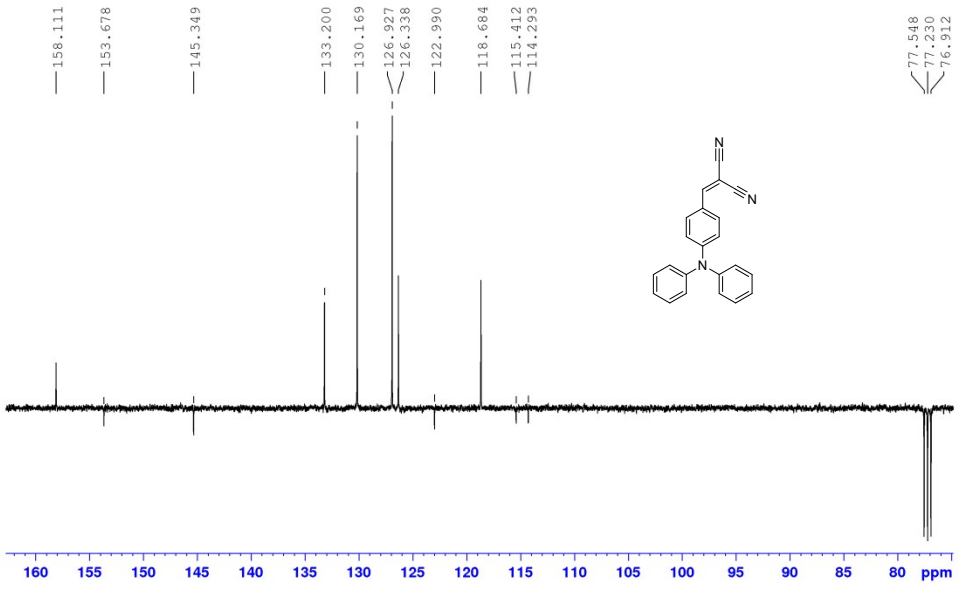

Figure S67. ^{13}C NMR APT spectrum of chromophore **9** (100 MHz, $CDCl_3$, 25 °C).

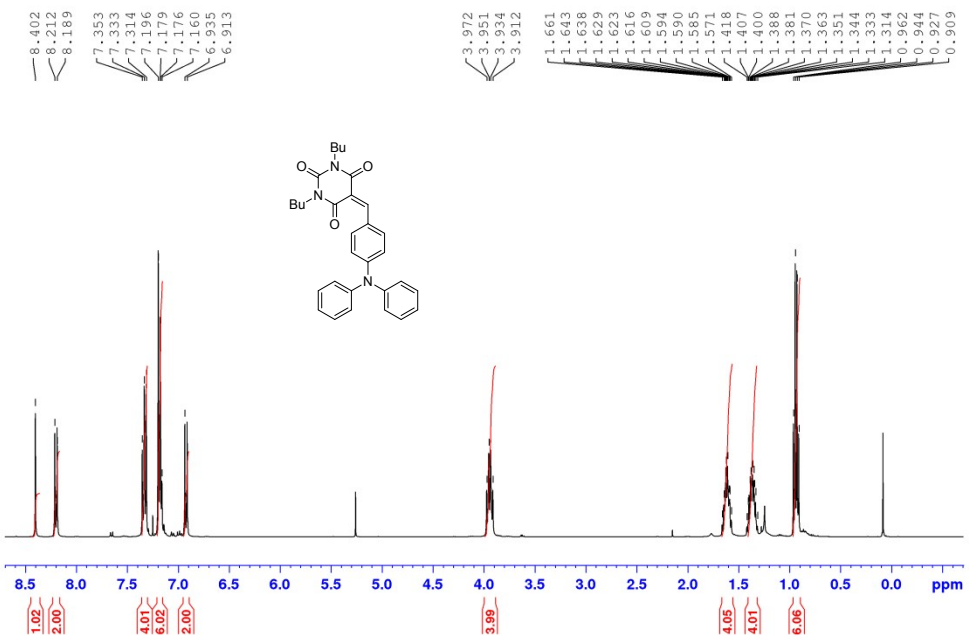

Figure S68. ^{1}H NMR spectrum of chromophore **10** (400 MHz, $CDCl_3$, 25 °C).

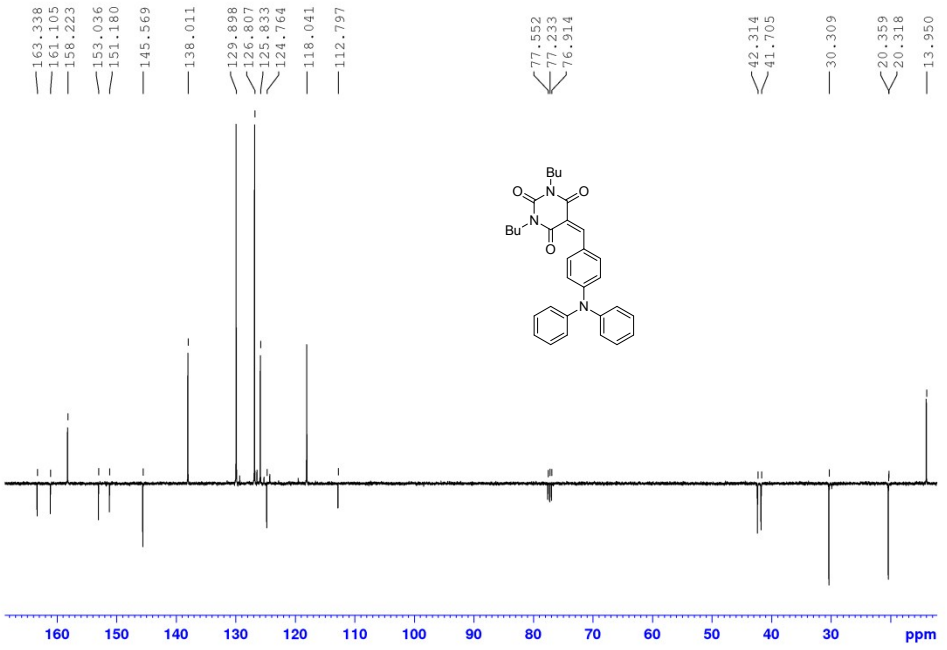

Figure S69. ^{13}C NMR APT spectrum of chromophore **10** (100 MHz, $CDCl_3$, 25 °C).

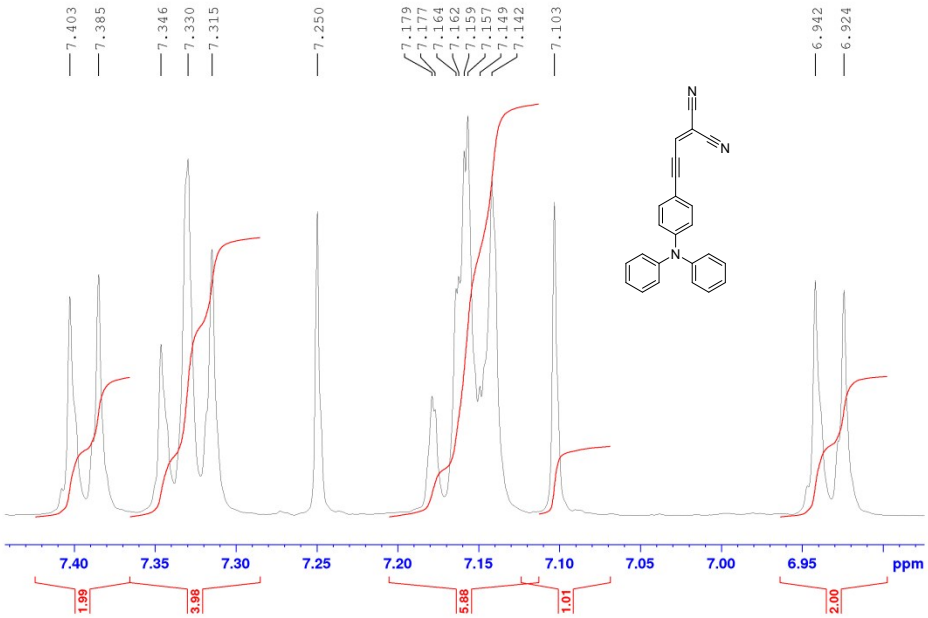

Figure S70. ^{1}H NMR spectrum of chromophore **11** (500 MHz, $CDCl_3$, 25 °C).

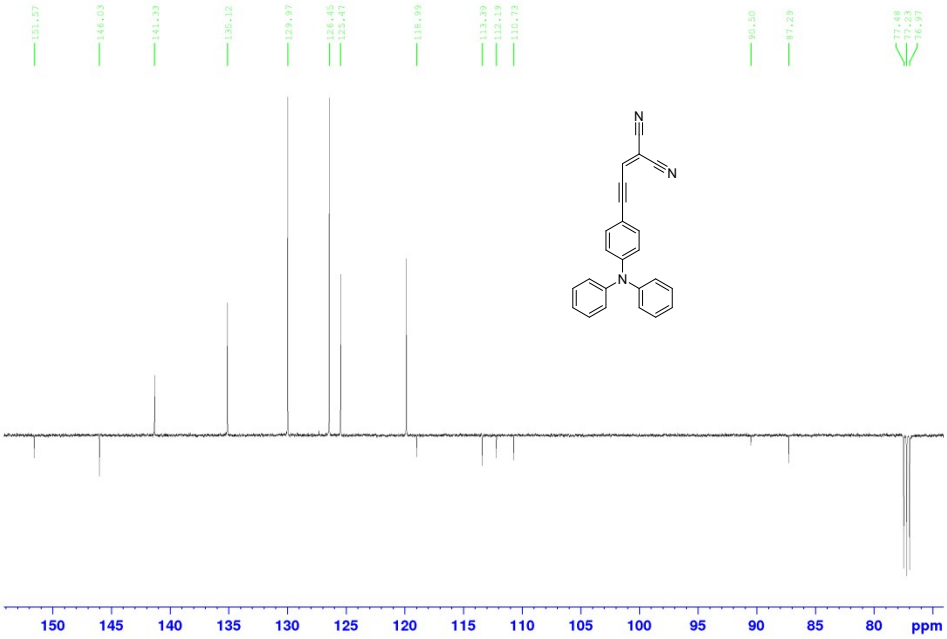

Figure S71. ^{13}C NMR APT spectrum of chromophore **11** (125 MHz, $CDCl_3$, 25 °C).

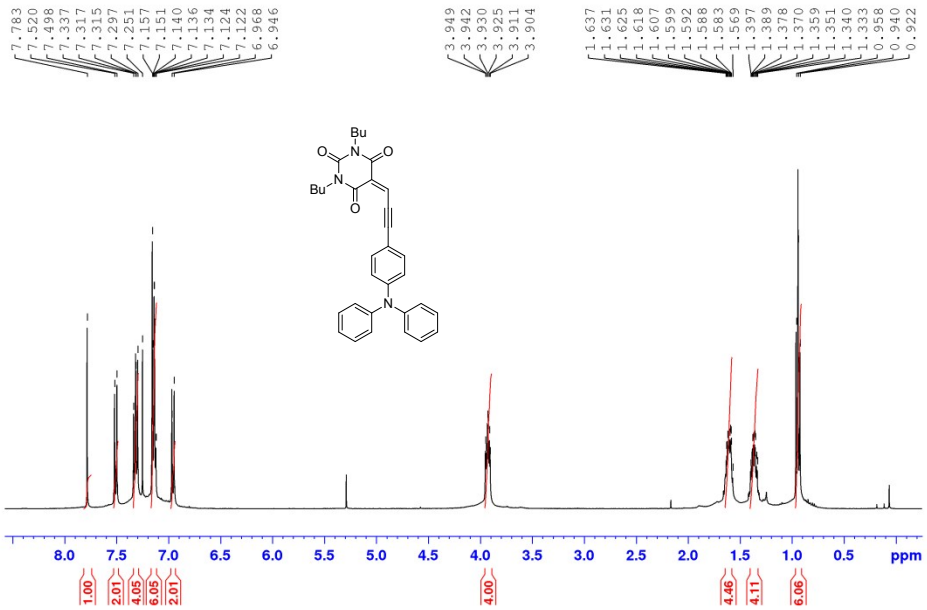

Figure S72. ^{1}H NMR spectrum of chromophore **12** (400 MHz, $CDCl_3$, 25 °C).

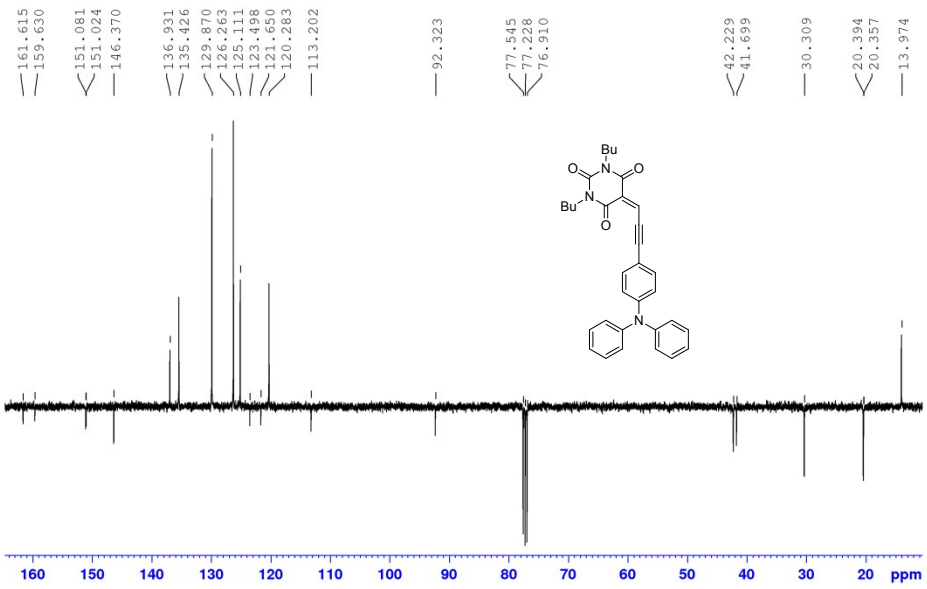

Figure S73. ^{13}C NMR APT spectrum of chromophore **12** (100 MHz, $CDCl_3$, 25 °C).

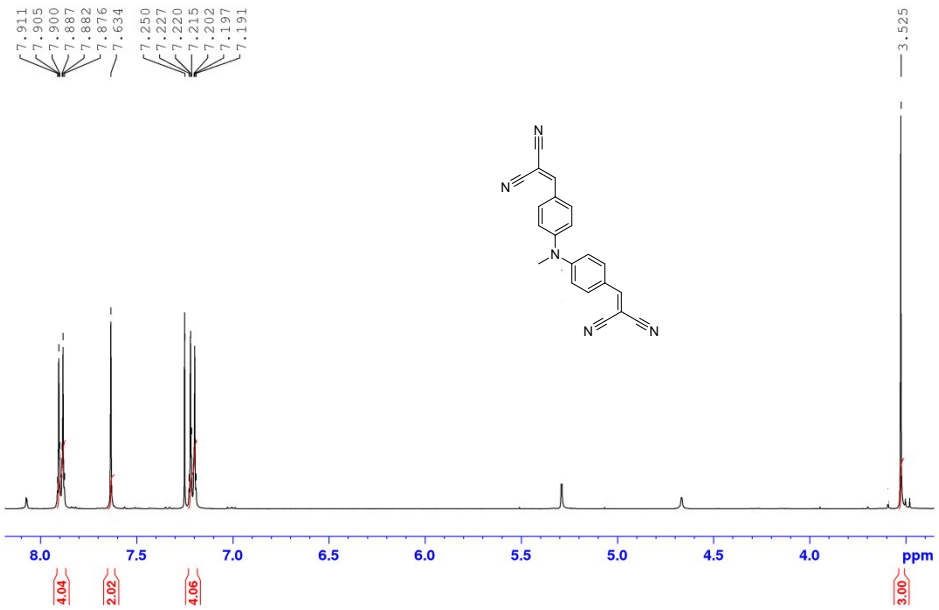

Figure S74. ^{1}H NMR spectrum of chromophore **13** (400 MHz, $CDCl_3$, 25 °C).

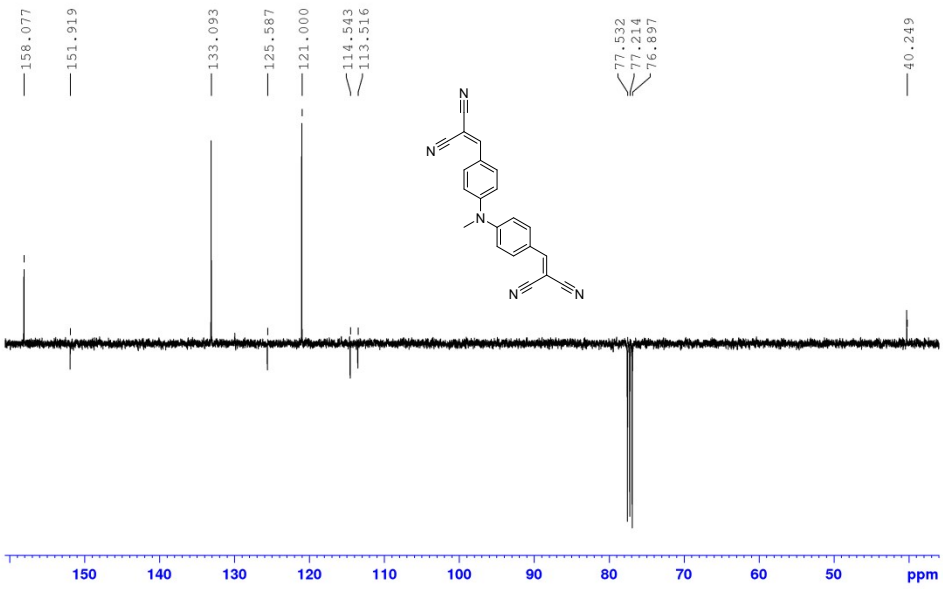

Figure S75. ^{13}C NMR APT spectrum of chromophore **13** (100 MHz, $CDCl_3$, 25 °C).

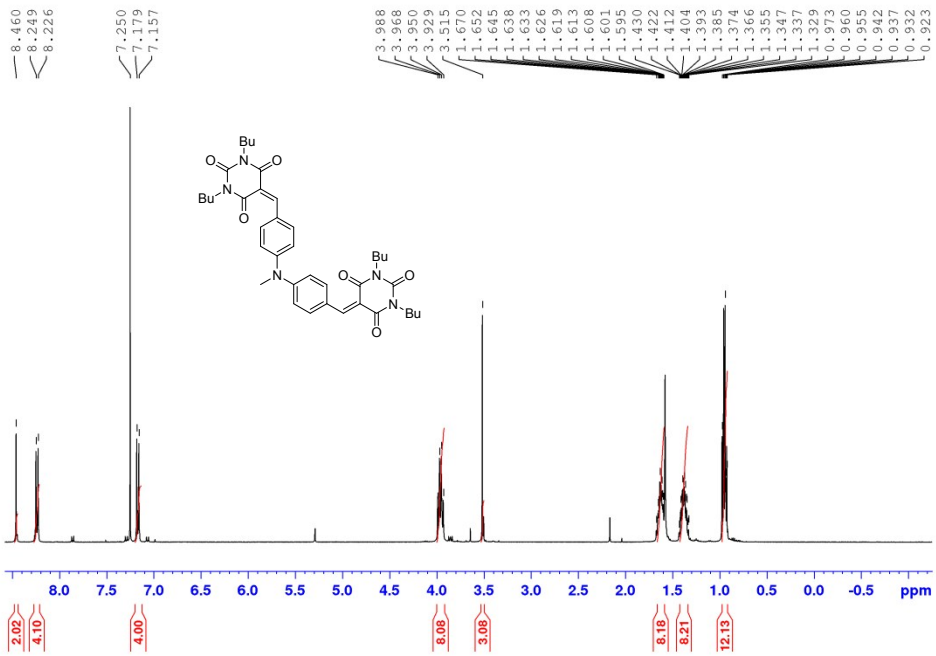

Figure S76. ^{1}H NMR spectrum of chromophore **14** (400 MHz, $CDCl_3$, 25 °C).

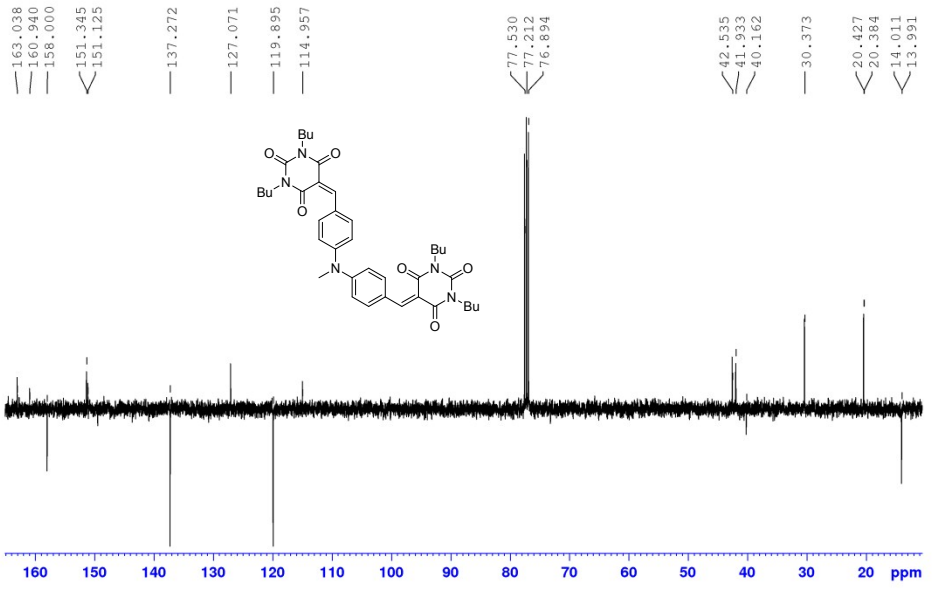

Figure S77. ^{13}C NMR APT spectrum of chromophore **14** (100 MHz, $CDCl_3$, 25 °C).

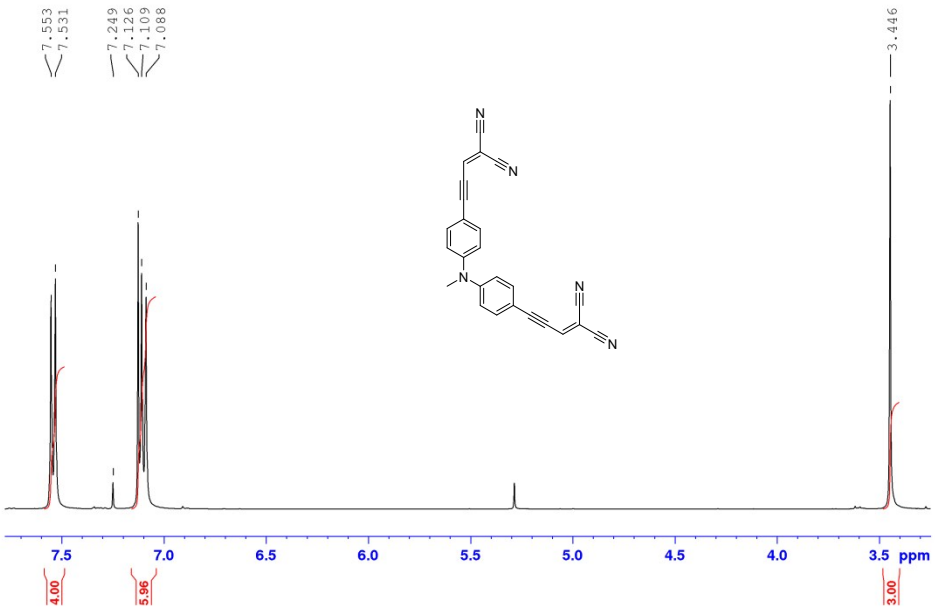

Figure S78. ^{1}H NMR spectrum of chromophore **15** (400 MHz, $CDCl_3$, 25 °C).

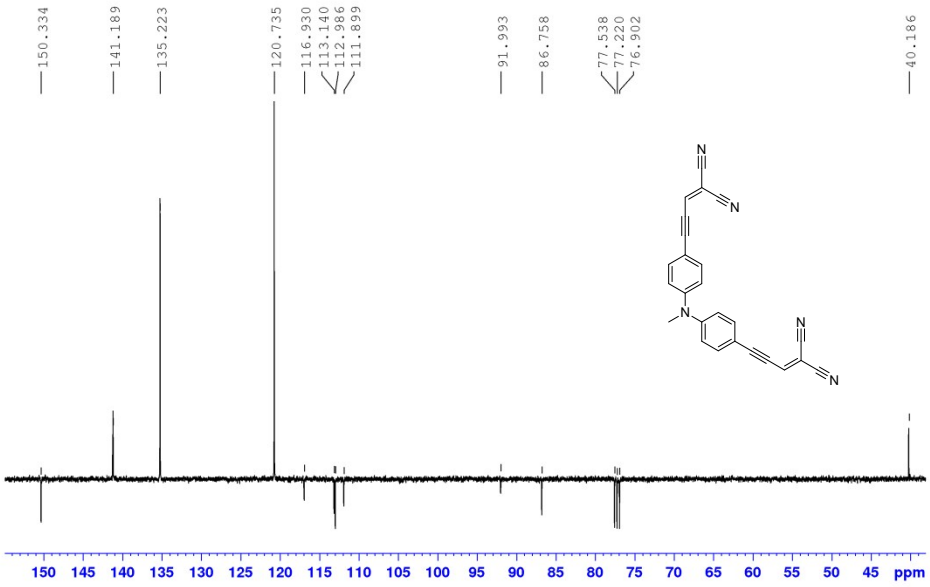

Figure S79. ^{13}C NMR APT spectrum of chromophore **15** (100 MHz, $CDCl_3$, 25 °C).

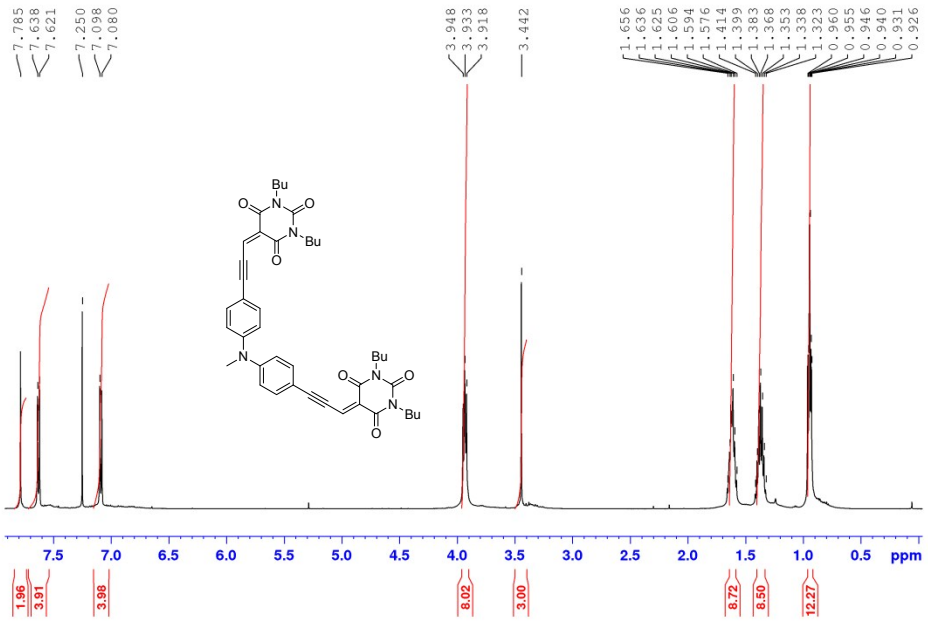

Figure S80. ^{1}H NMR spectrum of chromophore **16** (500 MHz, $CDCl_3$, 25 °C).

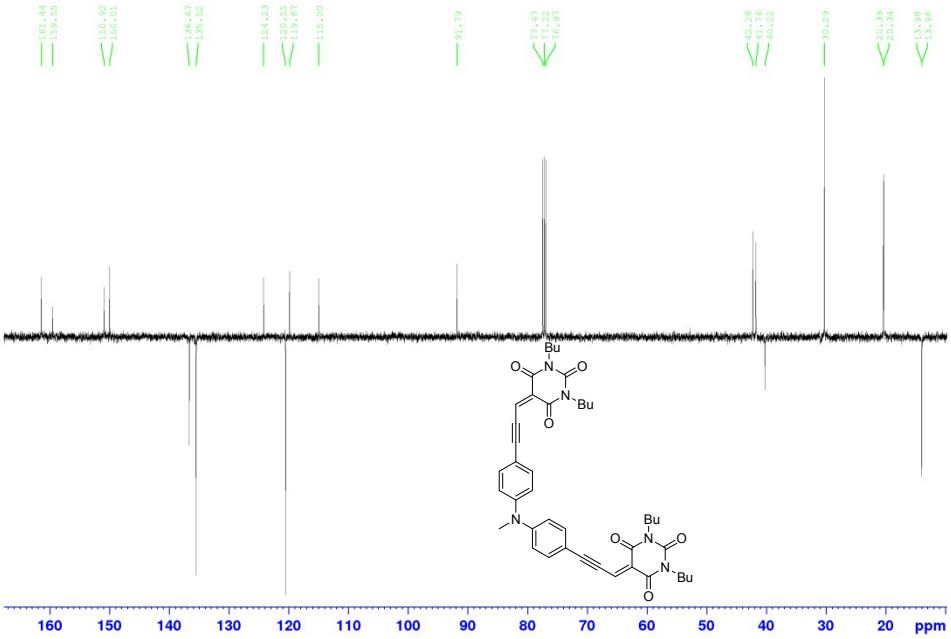

Figure S81. ^{13}C NMR APT spectrum of chromophore **16** (125 MHz, $CDCl_3$, 25 °C).

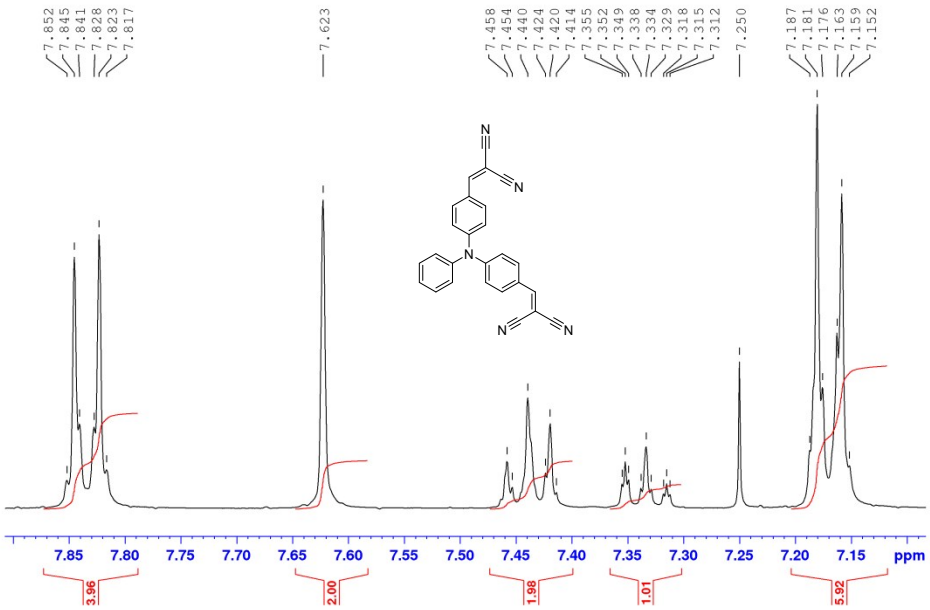

Figure S82. ^{1}H NMR spectrum of chromophore **17** (400 MHz, $CDCl_3$, 25 °C).

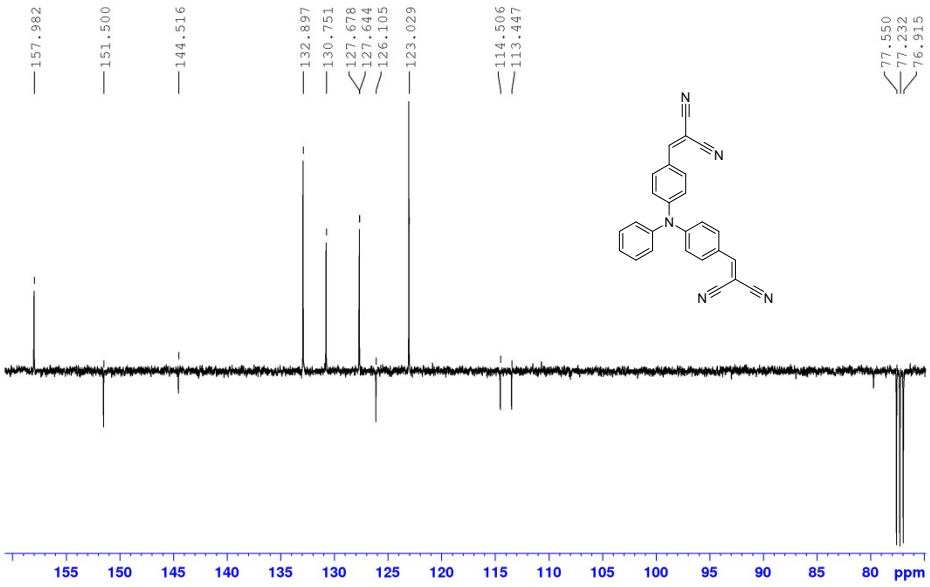

Figure S83. ^{13}C NMR APT spectrum of chromophore **17** (100 MHz, $CDCl_3$, 25 °C).

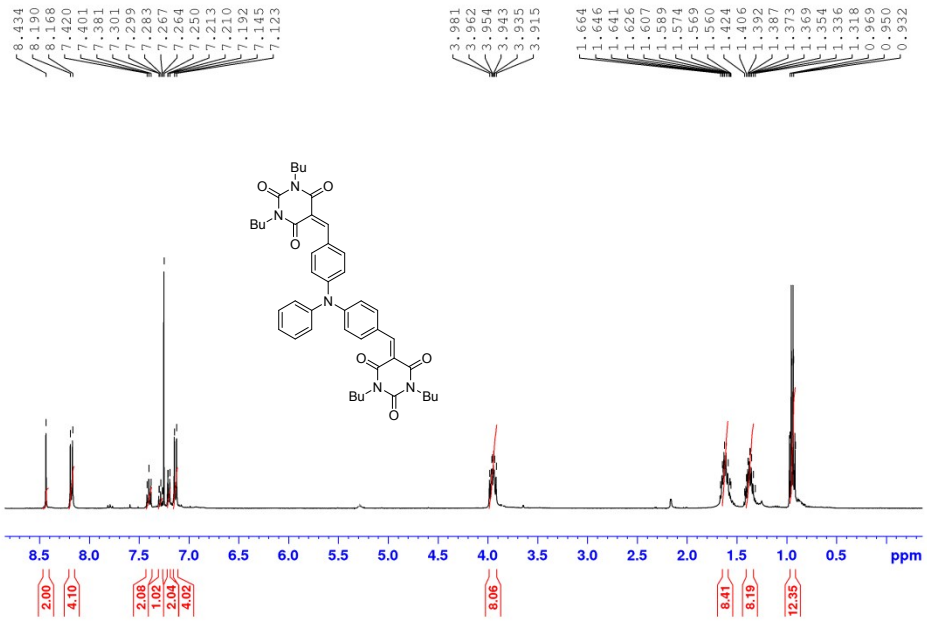

Figure S84. ^{1}H NMR spectrum of chromophore **18** (400 MHz, $CDCl_3$, 25 °C).

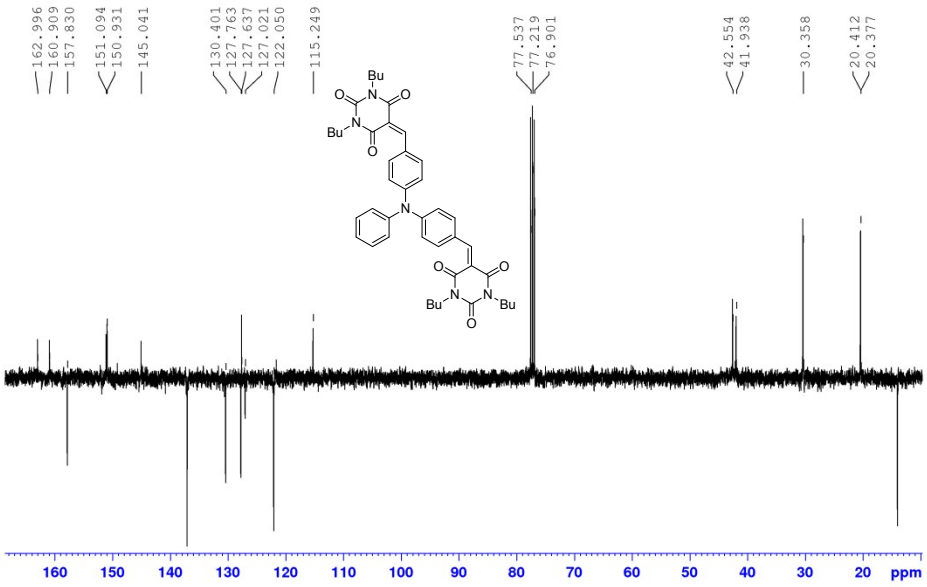

Figure S85. ^{13}C NMR APT spectrum of chromophore **18** (100 MHz, $CDCl_3$, 25 °C).

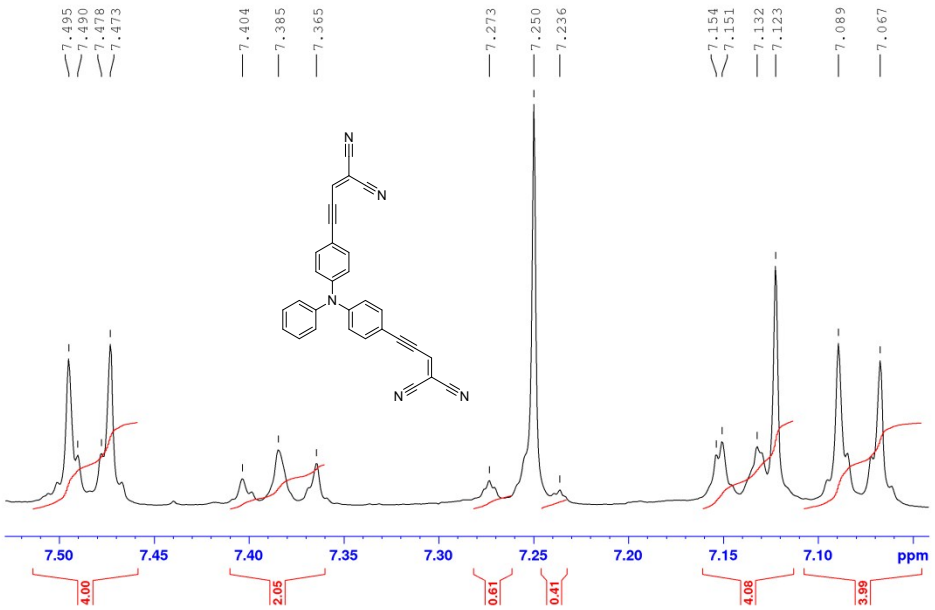

Figure S86. ^{1}H NMR spectrum of chromophore **19** (400 MHz, $CDCl_3$, 25 °C).

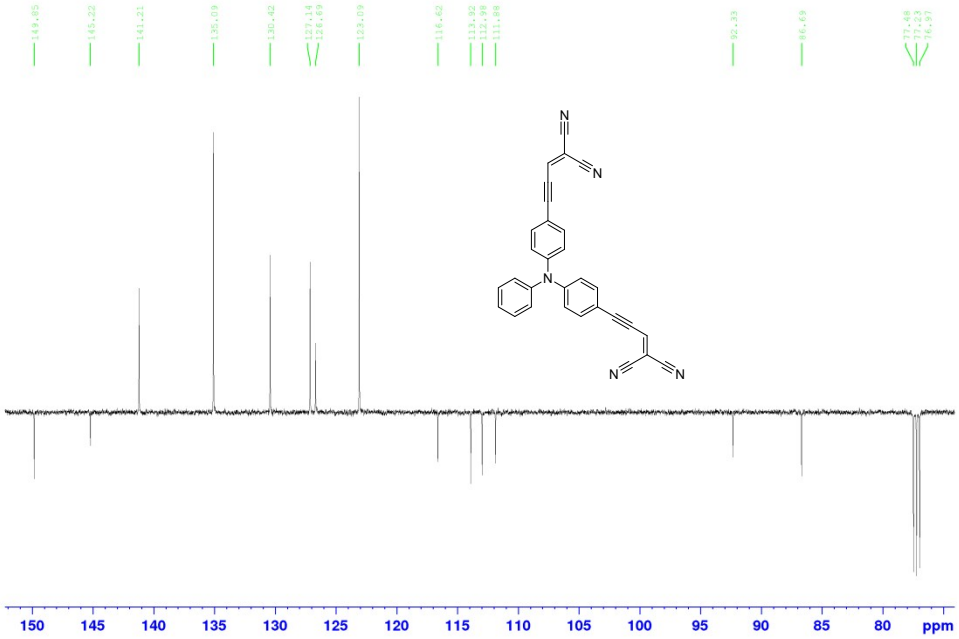

Figure S87. ^{13}C NMR APT spectrum of chromophore **19** (125 MHz, $CDCl_3$, 25 °C).

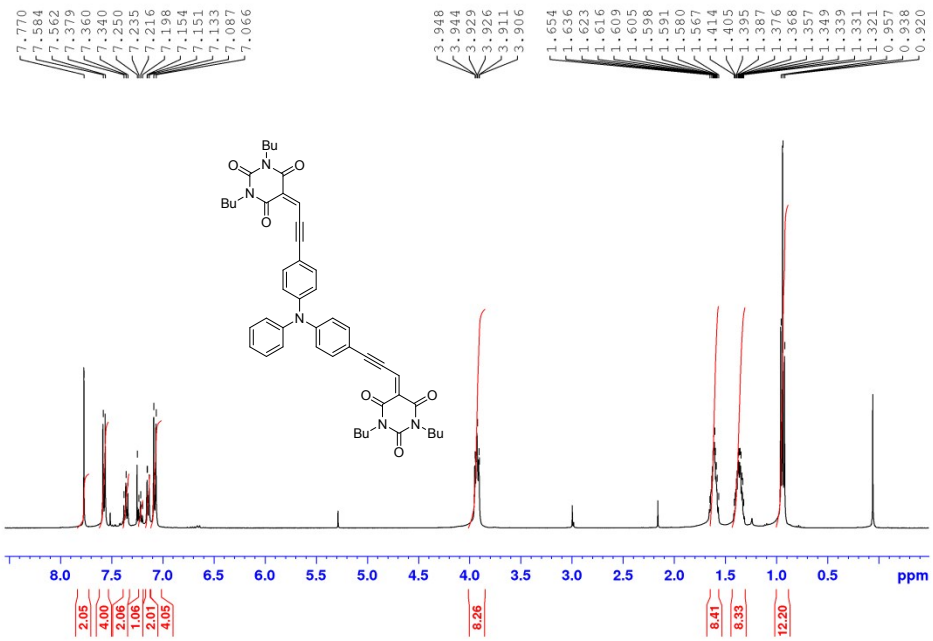

Figure S88. ^{1}H NMR spectrum of chromophore **20** (400 MHz, $CDCl_3$, 25 °C).

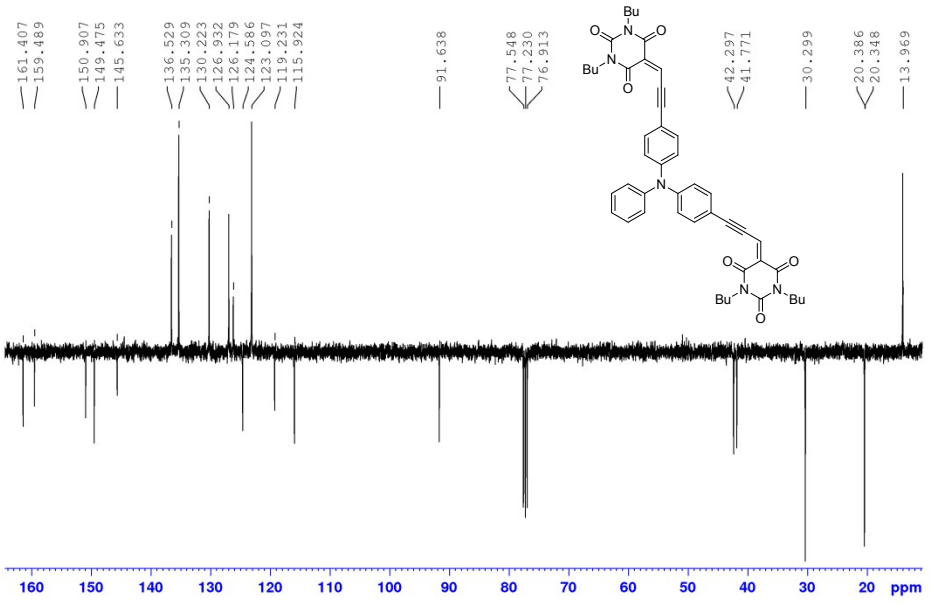

Figure S89. ^{13}C NMR APT spectrum of chromophore **20** (100 MHz, $CDCl_3$, 25 °C).

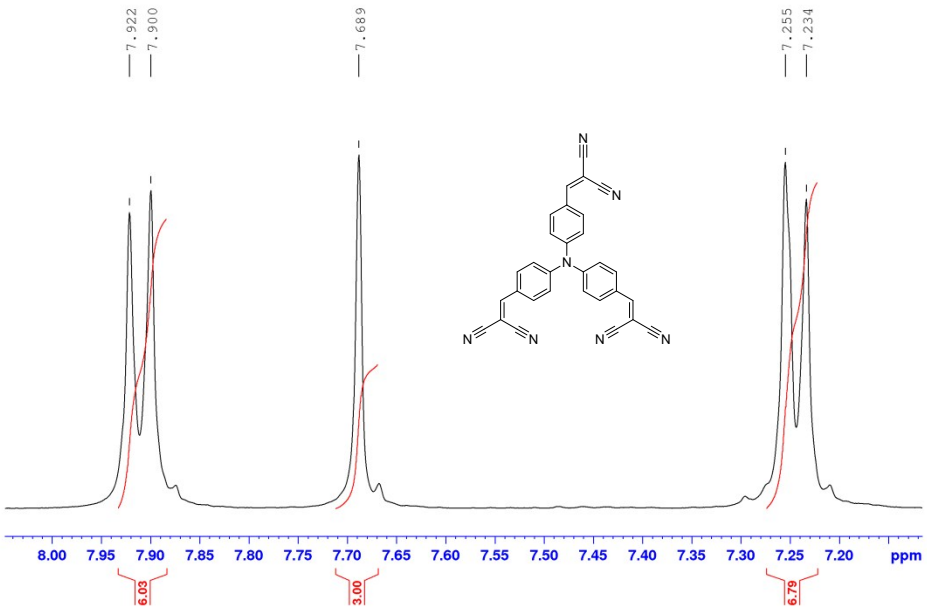

Figure S90. ^{1}H NMR spectrum of chromophore **21** (400 MHz, $CDCl_3$, 25 °C).

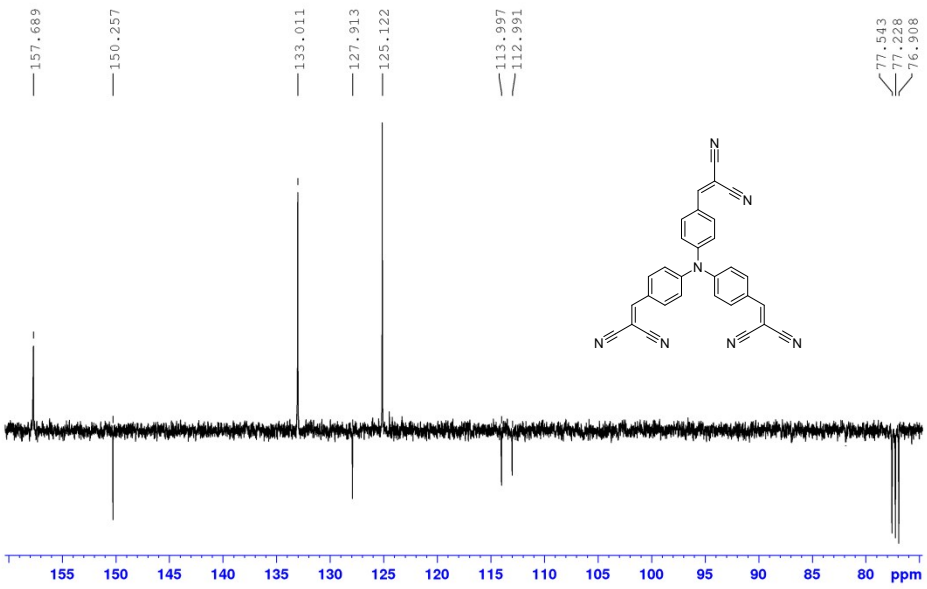

Figure S91. ^{13}C NMR APT spectrum of chromophore **21** (100 MHz, $CDCl_3$, 25 °C).

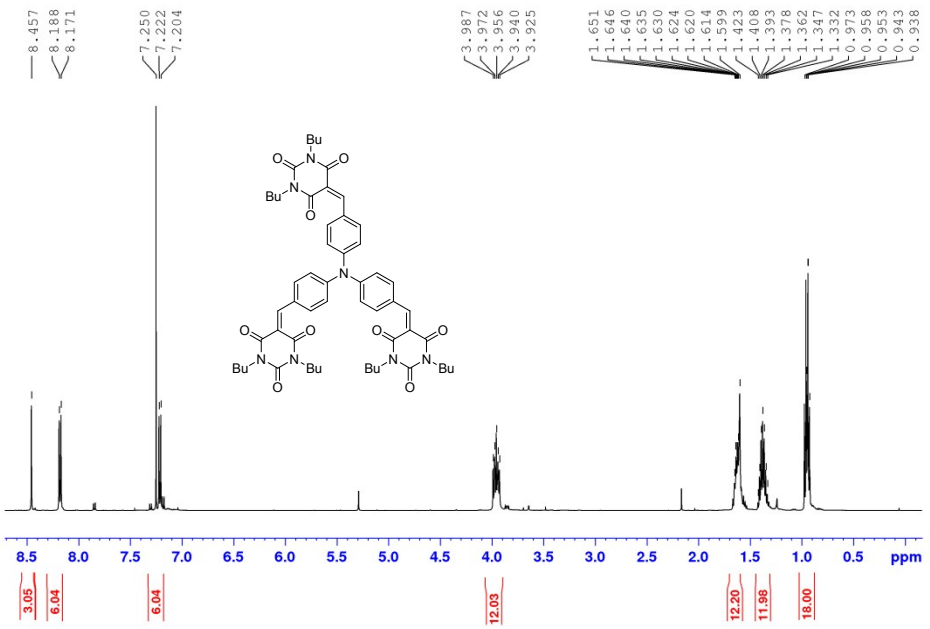

Figure S92. ^{1}H NMR APT spectrum of chromophore **22** (500 MHz, $CDCl_3$, 25 °C).

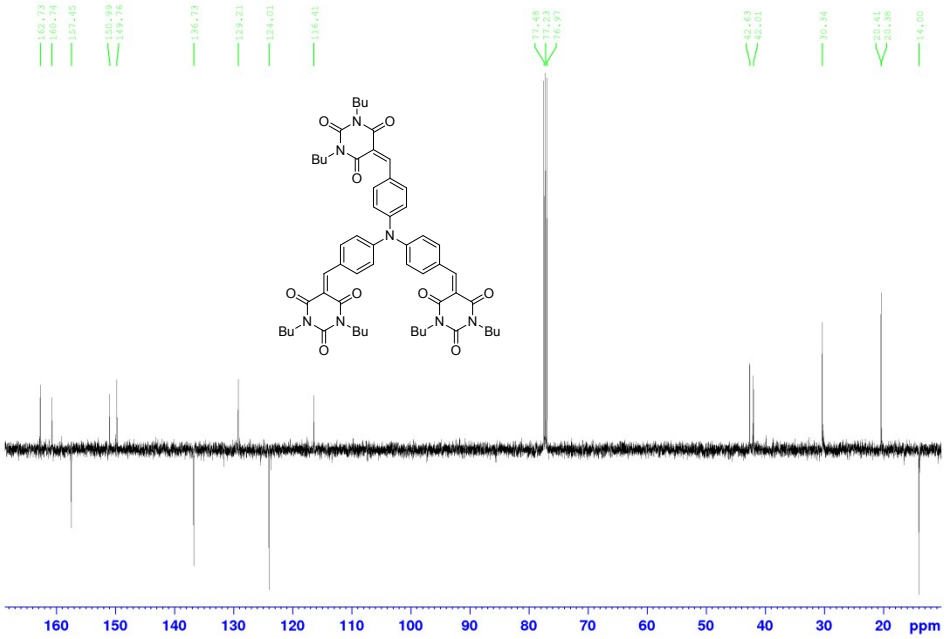

Figure S93. ^{13}C NMR spectrum of chromophore **22** (125 MHz, $CDCl_3$, 25 °C).

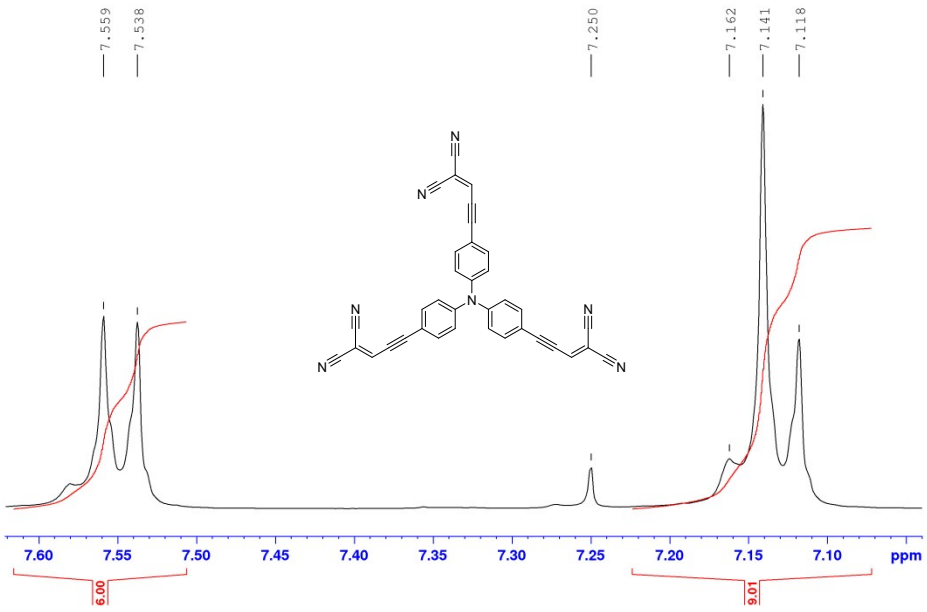

Figure S94. ^{1}H NMR spectrum of chromophore **23** (400 MHz, $CDCl_3$, 25 °C).

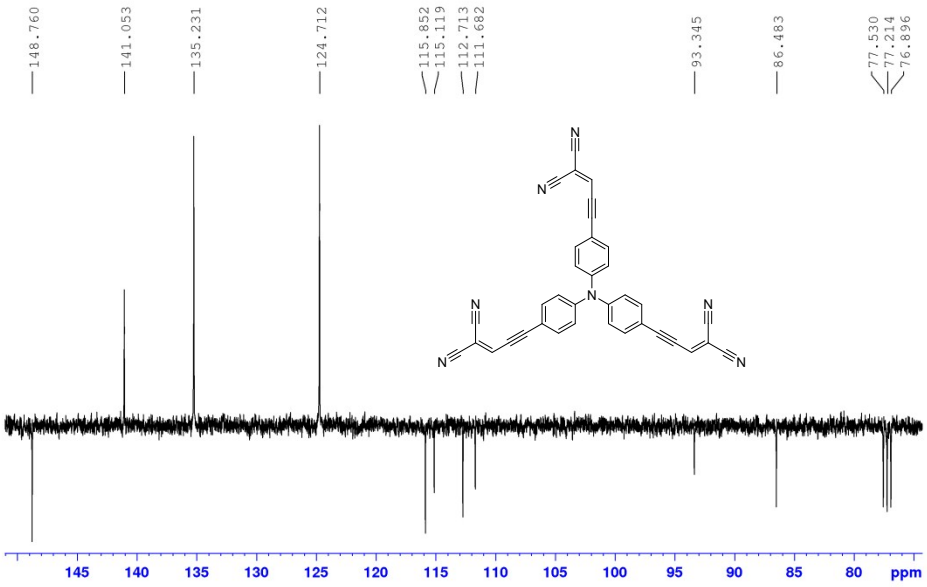

Figure S95. ^{13}C NMR APT spectrum of chromophore **23** (100 MHz, $CDCl_3$, 25 °C).

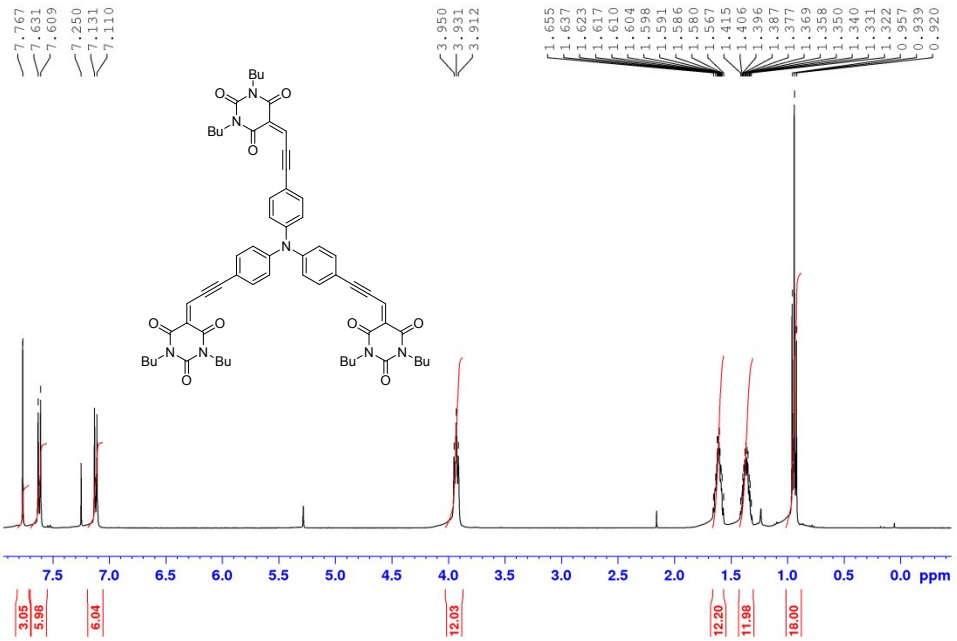

Figure S96. ^{1}H NMR spectrum of chromophore **24** (400 MHz, $CDCl_3$, 25 °C).

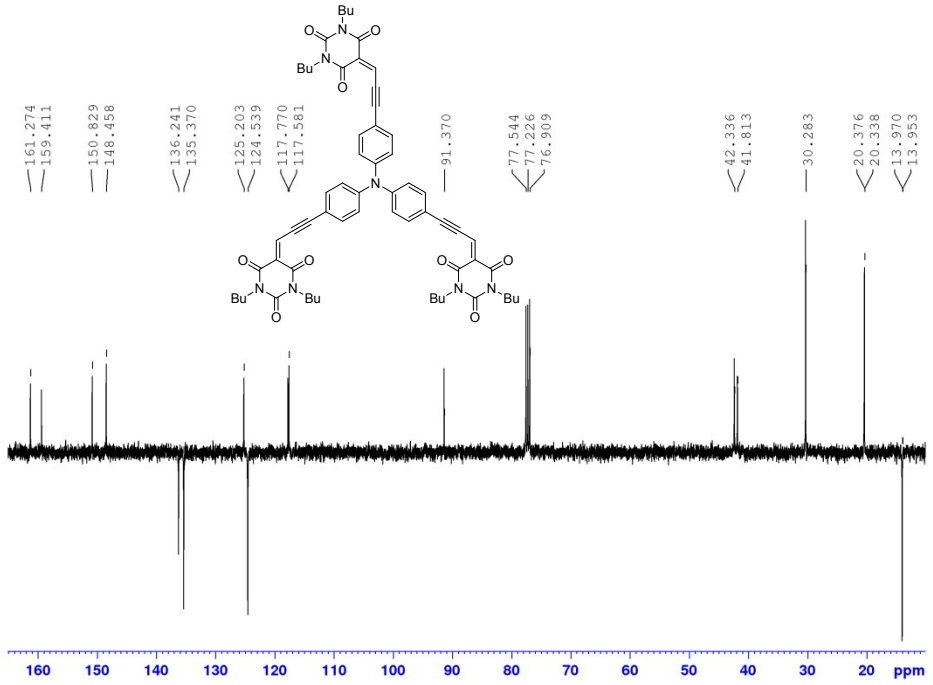

Figure S97. ^{13}C NMR APT spectrum of chromophore **24** (100 MHz, $CDCl_3$, 25 °C).

9. References

1. a) J. Sutharsan, D. Lichlyter, N. E. Wright, M. Dakanali, M. A. Haidekker, E. A. Theodorakis, *Tetrahedron*, **2010**, *66*, 2582-2588; b) M. Cui, M. Ono, H. Watanabe, H. Kimura, B. Liu, H. Saji, *J. Am. Chem. Soc*., **2014**, *136*, 3388-3394; c) S. Das, S. Sen, P. K. Bharadwaj, *Inorg. Chim. Acta*, **2011**, *372*, 425-428.

2. M. Klikar, F. Bureš, O. Pytela, T. Mikysek, Z. Padělková, A. Barsella, K. Dorkenoo, S. Achelle, *New J. Chem*., **2013**, *37*, 4230-4240.

3. T. Michinobu, J. C. May, J. H. Lim, C. Boudon, J.-P. Gisselbrecht, P. Seiler, M. Gross, I. Biaggio, F. Diederich, *Chem. Commun*., **2005**, *6*, 737-739.

4. a) X. Tang, W. Liu, J. Wu, Ch.-S. Lee, J. You, P. Wang, *J. Org. Chem*., **2010**, *75*, 7273-7278; e) F. Zhou, J. Shao, Y. Yang, J. Zhao, H. Guo, X. Li, S. Ji, Z. Zhang, *Eur. J. Org. Chem*., **2011**, *25*, 4773-4787; b) X. Li, Y.-A. Son, Y.-S. Kim, S.-H. Kim, J. Kun, J. Shin, *J. Nanosci. Nanotechnol*., **2012**, *12*, 1497-1502; c) X. Yang, X. Chen, X. Lu, C. Yan, Y. Xu, X. Hang, J. Qu, R. Liu, *J. Mater. Chem. C*, **2016**, *4*, 383-390.

5. C. Lambert, W. Gaschler, E. Schmälzlin, K. Meerholz, C. Bräuchle, *J. Chem. Soc., Perkin Trans*., **1999**, 577-587.

6. a) R. Lartia, C. Allain, G. Bordeau, F. Schmidt, C. Fiorini-Debuisschert, F. Charra, M.-P. Teulade-Fichou, *J. Org. Chem*., **2008**, *73*, 1732-1744; b) D. Cvejn, E. Michail, I. Polyzos, N. Almonasy, O. Pytela, M. Klikar, T. Mikysek, V. Giannetas, M. Fakis, F. Bureš, *J. Mater. Chem. C* **2015**, *3*, 7345-7355.

7. J. Shao, S. Ji, X. Li, J. Zhao, F. Zhou, H. Guo, *Eur. J. Org. Chem*., **2011**, *30*, 6100-6109.

8. M. S. Yosubov, E. N. Tveryakova, E. A. Krasnokutskaya, I. A. Perederyna, V. V. Zhdankin, *Synth. Commun*., **2007**, *37*, 1259-1265.

9. a) J. Freudenberg, F. Rominger, U. H. F. Bunz, *Chem. Eur. J*., **2015**, *21*, 16749-16753; b) S. S. Bhojgude, T. Kaicharla, A. T. Biju, *Org. Lett*., **2013**, *15*, 5452-5455.

10. J.-K. Fang, D.-L. An, K. Wakamatsu, T. Ishikawa, T. Iwanaga, S. Toyota, D. Matsuo, A. Orita, J. Otera, *Tetrahedron Lett*., **2010**, *51*, 917-920.

11. S. Akiyama, S. Nakatsuji, K. Yoshida, K. Nakashima, T. Hagiwara, *Bull. Chem. Soc. Jpn*., **1983**, *56*, 361-362.

12. Gaussian 09, Revision D.01, M. J. Frisch, G. W. Trucks, H. B. Schlegel, G. E. Scuseria, M. A. Robb, J. R. Cheeseman, G. Scalmani, V. Barone, B. Mennucci, G. A. Petersson, H. Nakatsuji, M. Caricato, X. Li, H. P. Hratchian, A. F. Izmaylov, J. Bloino, G. Zheng, J. L. Sonnenberg, M. Hada, M. Ehara, K. Toyota, R. Fukuda, J. Hasegawa, M. Ishida, T. Nakajima, Y. Honda, O. Kitao, H. Nakai, T. Vreven, J. A. Montgomery, Jr., J. E. Peralta, F. Ogliaro, M. Bearpark, J. J. Heyd, E. Brothers, K. N. Kudin, V. N. Staroverov, T. Keith, R. Kobayashi, J. Normand, K. Raghavachari, A. Rendell, J. C. Burant, S. S. Iyengar, J. Tomasi, M. Cossi, N. Rega, J. M. Millam, M. Klene, J. E. Knox, J. B. Cross, V. Bakken, C. Adamo, J. Jaramillo, R. Gomperts, R. E. Stratmann, O. Yazyev, A. J. Austin, R. Cammi, C. Pomelli, J. W. Ochterski, R. L. Martin, K. Morokuma, V. G. Zakrzewski, G. A. Voth, P. Salvador, J. J. Dannenberg, S. Dapprich, A. D. Daniels, O. Farkas, J. B. Foresman, J. V. Ortiz, J. Cioslowski, D. J. Fox, Gaussian, Inc., Wallingford CT, **2013**.

13. ArgusLab 4.0, Mark A. Thompson, Planaria Software LLC, Seattle, WA. http://www.arguslab.com

14. MOPAC2012, J. J. P. Stewart, Stewart Computational Chemistry, version 13.084W, webpage: http://OpenMOPAC.net.

15. OPChem, O. Pytela, version 7.6, webpage: http://pytela.upce.cz/OPgm.